NOTCH FILTER CONTROL OF MAGNETIC BEARINGS TO IMPROVE ROTOR SYNCHRONOUS RESPONSE

by

REINHARD BEATTY

S.B., Mechanical Engineering
Massachusetts Institute of Technology
(1985)

Submitted to the Department of Mechanical Engineering
in Partial Fulfillment of the
Requirements for the Degree of

MASTER OF SCIENCE IN MECHANICAL ENGINEERING

at the

MASSACHUSETTS INSTITUTE OF TECHNOLOGY

May 1988

Signature of Author: _____
Department of Mechanical Engineering
May 27, 1988

Approved by: _____
Dr. Bruce G. Johnson
Technical Supervisor, SatCon Technology Corp

Certified by: _____
Professor Derek Rowell
Thesis Supervisor

Accepted by: _____
Professor Ain Sonin
Chairman, Department Graduate Committee

NOTCH FILTER CONTROL OF MAGNETIC BEARINGS TO IMPROVE ROTOR SYNCHRONOUS RESPONSE

by

REINHARD BEATTY

Submitted to the Department of Mechanical Engineering on May 6, 1988 in partial fulfillment of the requirements for the Degree of Master of Science in Mechanical Engineering

ABSTRACT

This thesis analytically examines the effects of a tracking notch filter controller on the stability and performance of active radial magnetic bearing systems. Previous research has shown that notch filter control of magnetic bearings helps reduce vibrations caused by mass imbalance of the rotor that occur at the rotational (synchronous) frequency. Furthermore, it has been shown that the notch filter causes the system to become unstable for rotational frequencies near critical frequencies of the system, i.e. loop crossover frequency or shaft resonant frequency. The goal of this thesis has been to gain a more thorough analytical understanding of the mechanism by which the tracking notch filter at the rotational frequency attenuates the synchronous vibrations caused by rotor imbalance and how the stability of the system changes with rotational frequency.

Three rotor models with centrally located rotor are examined with respect to their translational dynamics. They are 1) rigid shaft, 2) Jeffcott rotor model (flexible shaft) with shaft relatively stiff compared to the bearings, and 3) Jeffcott rotor model with shaft relatively soft compared to the bearings. Control systems for these models employ feedback of bearing position. Rotor position feedback is also examined for the third model, assuming no spillover effects. The results show that the notch filter causes the system to become unstable over a range of rotational frequencies below the lowest system critical frequency. The notch filter can be used to attenuate the synchronous disturbance without causing instability for rotational frequencies above the lowest system critical frequency.

Thesis Supervisor: Dr. Derek Rowell

Title: Professor of Mechanical Engineering

ACKNOWLEDGEMENTS

I would like to express my appreciation to Bruce Johnson for providing technical supervision and for making time to direct my progress whenever I needed advice. Bruce's technical expertise and background in the field of magnetic bearing control were invaluable to me. I would like to thank Professor Derek Rowell for supervising this thesis; it was a pleasure working with Professor Rowell. I would also like to thank David Eisenhaure for placing the resources of SatCon Technology Corporation at my disposal. This thesis has also benefitted enormously from the people and experience available at SatCon. I appreciate the time and effort that was required in reviewing, criticizing and advising my work there.

I feel fortunate to have been part of General Electric Company's Advanced Course in Engineering. This thesis would not have been possible without the financial support and time off from work which GE provided me.

TABLE OF CONTENTS

List of Figures

CHAPTER 1
INTRODUCTION AND BACKGROUND

Because of their many advantages over conventional ball or roller bearings, applications are increasingly being found for actively controlled magnetic bearings. Since magnetic bearings suspend the rotating structure without contact, no friction is present and the absence of bearing surface wear gives greatly extended reliability. In many applications, the power needed to levitate the shaft is negligible compared to the energy consumed by friction in conventional bearings. Furthermore, magnetic bearings eliminate the need for lubrication systems which cannot be used in hostile environments of extreme temperatures or pressures. Perhaps most importantly, since the rotor is actively suspended, the dynamic behavior of the bearing can be customized to suit the requirements of the particular application.

The most common magnetic bearings consist of an array of closely spaced electromagnets, each imposing an attractive force on the rotor. The combined force is adjusted, based on the rotor position, to maintain the air gap between rotor and stator. Small inductive sensors provide the position signal. Using local feedback, where the bearing force is a function of the position time-history at the bearing, the dynamic behavior can be made similar to that of a conventional bearing. The actively controlled magnetic bearing can produce stiffness and damping forces proportional to the position and velocity of the rotor at the bearing, just as conventional bearings do.

The use of magnetic levitation to suspend rotating bodies, although not a new idea, has been made possible by the advent of control system theory. The earliest magnetic bearings were used in conjunction with conventional bearings because magnetic bearings are inherently unstable by themselves [Geary 1964]. It was predicted earlier by

Earnshaw that two bodies could not be statically stable if the attractive force between them varies as the inverse of the square of the distance separating them [Earnshaw 1842], as does the ferromagnetic force. It was later shown that feedback control of any unstable translational axes could result in stable suspension [Beams 1946].

The type of feedback control used for a bearing depends on the requirements of the application. When axial position must be closely controlled, an active axial bearing is used, as shown in Figure 1.1. The magnets in the stator act on a disk perpendicular to the shaft to maintain the axial air gap. This type of bearing is radially passive: radial stability is provided by the arrangement of the fringing rings, relying on the natural tendency of the rotor and stator to align themselves. Since the rings are unstable in the axial direction, they must be actively controlled in this axis.

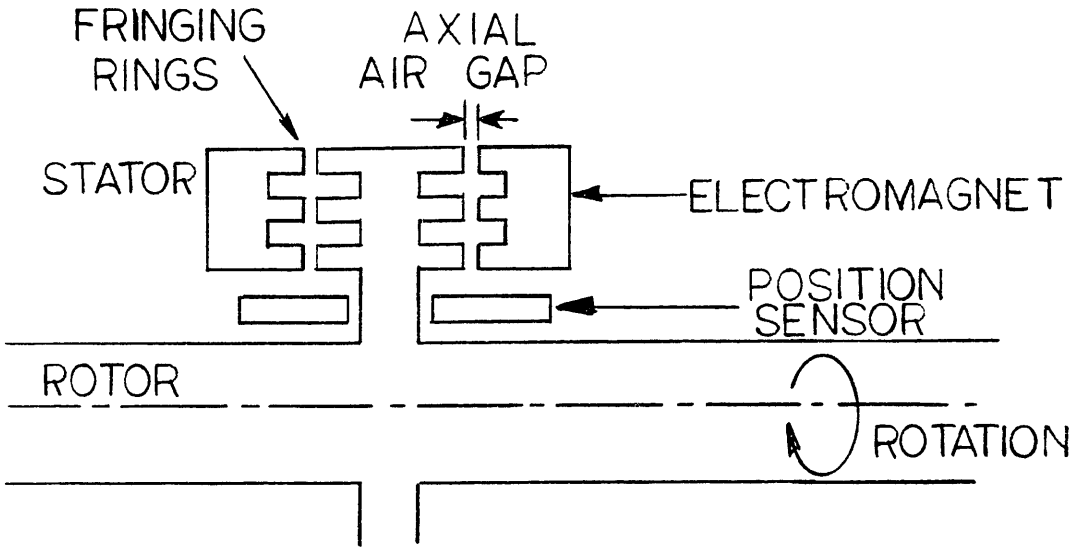

Figure 1.1 Active Axial, Passive Radial Magnetic Bearing

Figure 1.2 shows a radially active bearing, used in supporting radial loads. Both the x and y radial axes must be actively controlled whereas the axial direction is passively stable.

A schematic diagram of a radially active bearing control loop is shown in Figure 1.3. The position sensor provides a signal to the controller which responds by countering the radial motion of the rotor with an appropriate control signal to the electromagnet. The electromagnet applies a force to the rotor proportional to the control signal, thus maintaining the air gap between the rotor and stator. Identical control loops exist for all four of the bearing electromagnets.

One application of active magnetic bearings, made possible by the flexibility of the control system, is in vibration control. Unlike conventional bearings, in which the stiffness and damping characteristics are closely linked by the physical characteristics of the bearing material, magnetic bearings may be given a wide range of

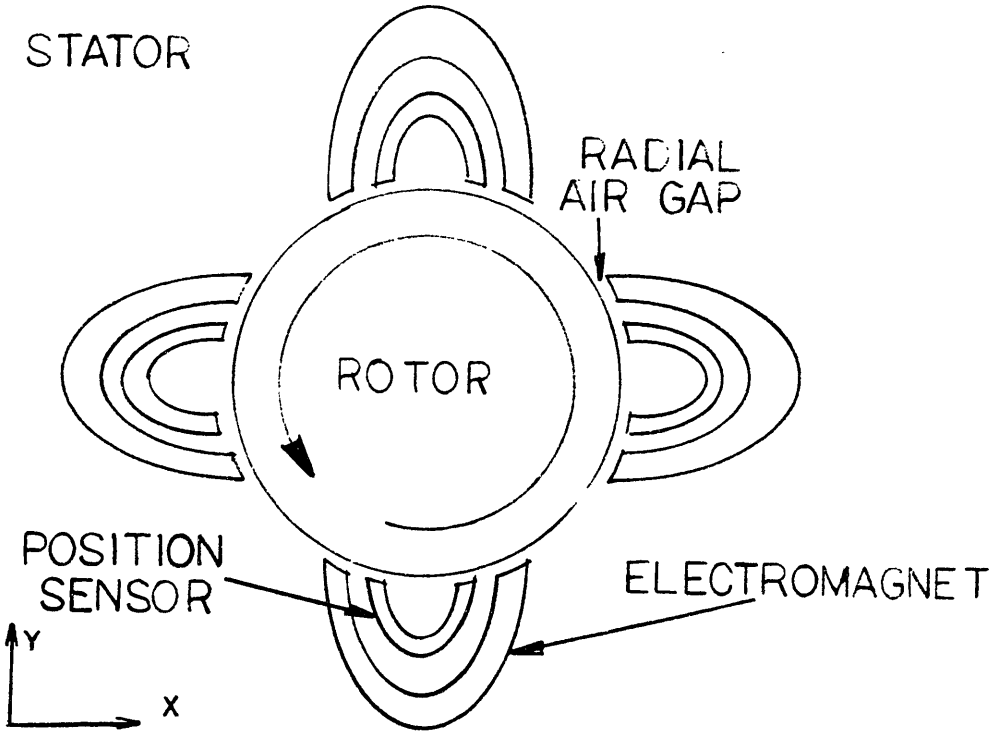

Figure 1.2 Active Radial, Passive Axial Magnetic Bearing

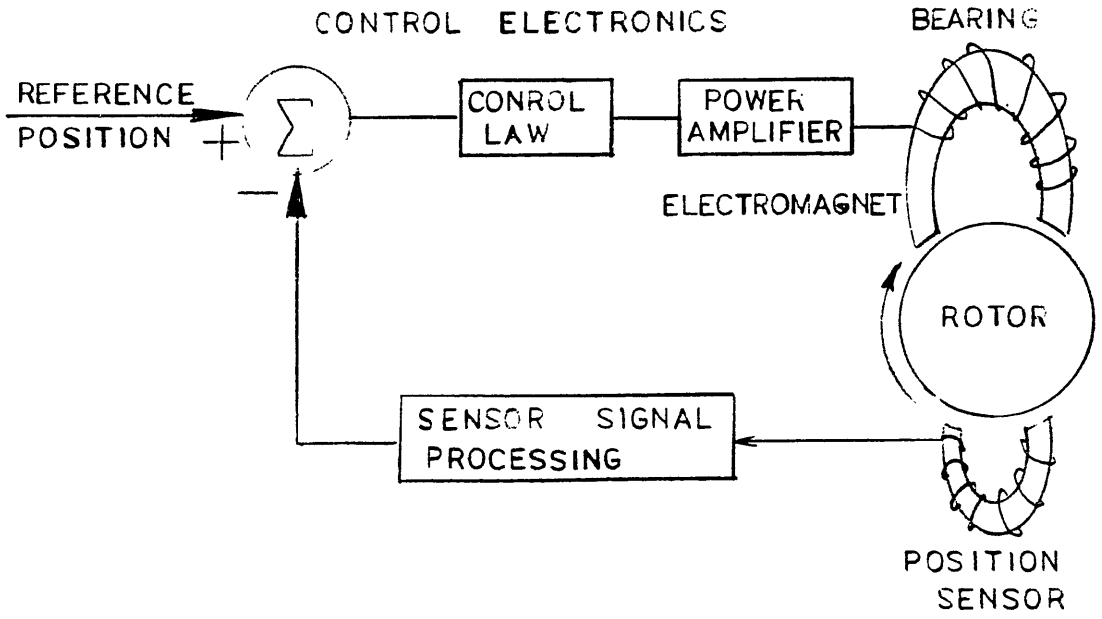

Figure 1.3 Active Radial Bearing Control Loop Schematic

different dynamic characteristics. For example, it has been demonstrated that active radial magnetic bearings mounted at the midspan of a transmission shaft can be effectively used as pure dampers to control radial vibrations of the shaft [Nikolajsen 1979].

A common cause of radial vibrations is rotor imbalance. No matter how accurately a rotor is machined, the inertial axis is never perfectly aligned with the geometric axis. When rotated freely, such a rotor naturally chooses to rotate about its inertial axis. However, when rotated on bearings, rotation is constrained to its geometric axis. Synchronous vibratory forces are then generated by the bearings and conducted to the stator structure.

In dealing with rotor imbalance, the approach to bearing design depends on the objective. For applications where precise rotation about the geometric axis is required, such as turbine rotors and precision lathes, rotor deflection can be limited by choosing extremely stiff

bearings. On the other hand, for some applications, such as flywheels, it may be more important to eliminate the vibratory forces transmitted by the bearings to the stator structure. This has been successfully accomplished by Societe De Mecanique Magnetique using actively controlled magnetic bearings [Habermann 1985]. The vibratory bearing forces are eliminated by selectively filtering out the position signal at the rotational speed, since this is the frequency of the vibration. Such a control loop with a tracking notch filter in the feedback path is shown in Figure 1.4. The effect of the filter is to eliminate bearing stiffness at the rotational speed, allowing the rotor to choose its rotational axis and rotate freely about its inertial axis. However, for any other frequency of disturbance, the bearing provides sufficient stiffness to maintain the air gap between rotor and stator and provide system stability.

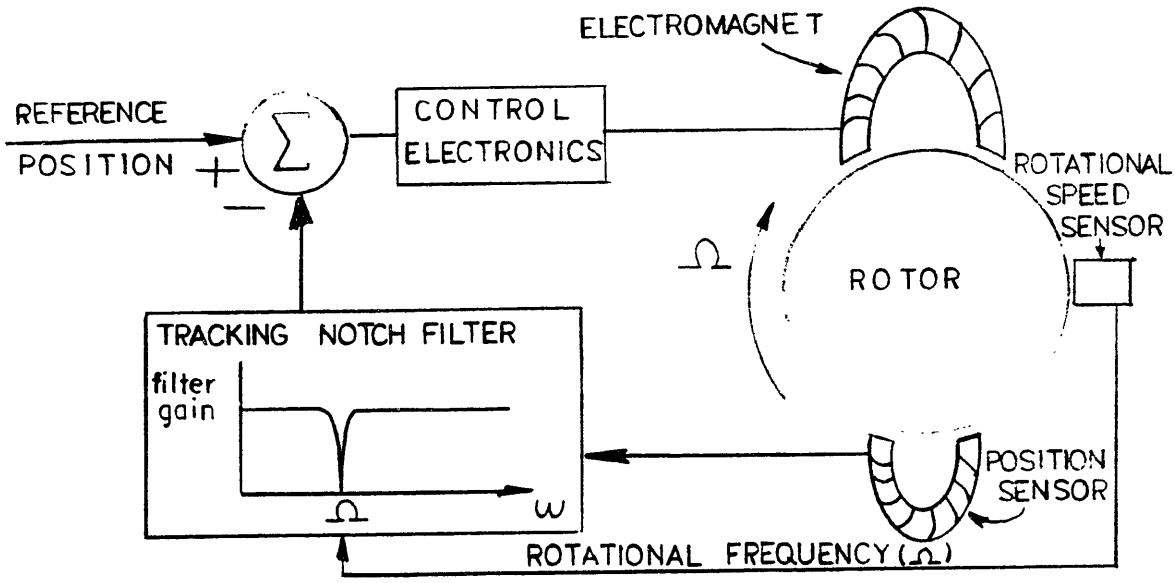

Figure 1.4 Vibration Control using Tracking Notch Filter

Active magnetic bearings with notch filters are currently being introduced to reduce the rotor synchronous vibrations. Tracking notch filters are used since they can act at any rotational speed, however, the notch filter must be disabled near rotor critical speeds, i.e. loop crossover frequency or shaft resonant frequency, in order to maintain stable operation. It can be surmised that the phase shift of the notch filter is responsible for the region of instability but the exact nature of the constraints placed on the controller design by the notch filter are unknown.

The objective of this thesis is to define the effect of the tracking notch filter on the stability and performance of an active radial magnetic bearing system. The approach taken is to model rigid and flexible rotors with a mass imbalance in Chapter 2. Control systems will be designed to allow active radial magnetic bearings to provide stable suspension of these plants and to give some generally desirable frequency response in Chapter 3. An attempt will be made to generalize the plant models and controller designs in order to make the results meaningful and applicable to a wide range of applications. Once reasonable systems have been developed, the tracking notch filter will be introduced in Chapter 4. Its effect on the system stability and the synchronous response of the system as a function of rotational speed will be studied in Chapters 5 and 6 respectively. The approach and results will be summarized and conclusions will be drawn in Chapter 7.

CHAPTER 2
MODEL DESCRIPTION

2.1. Rigid Rotor Model

Simplification of the synchronous response problem to its most basic form is desirable because results are easily attainable and may be applied directly to more complex models. The simplest model of rotor imbalance is a rotor of mass m mounted on a rigid massless shaft. Such a model is shown in Figure 2.1. The rotor geometric center joins the plane of the rotor at point S and is offset from the rotor center of mass (M) by a distance ϵ. Bearing forces, $F_b/2$, act on the shaft ends and are assumed to be identical.

Complex coordinates are used here to describe the location of a point in the x-y plane using a single variable as follows:

$$Z = x + iy \qquad 2.1$$

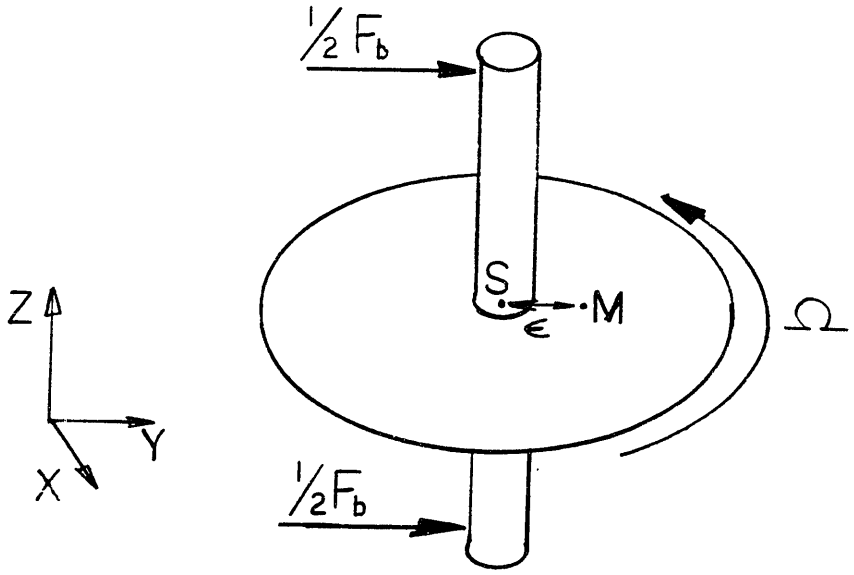

Figure 2.1. Rigid Rotor Model Geometry

where x and y represent the x and y coordinates of the point. As a result of this conversion, half as many equations are required to completely describe the system.

From Newton's second law, the position of the center of mass may be written directly as:

$$Z_m = F_b/(ms^2) \qquad 2.2$$

where Z_m is the complex coordinate of point M, s is the complex Laplace variable, and Fb is the complex force the bearings apply to the shaft. Since the shaft is assumed to be massless, the force applied by the bearings is identical to the force the shaft applies to the rotor. The rotor position can be written relative to the mass center as:

$$Z_s = Z_m + \epsilon e^{j\Omega t} \qquad 2.3$$

where ϵ is the mass imbalance distance, as previously stated, and Ω is the rotational speed of the rotor. By ignoring the synchronous term in equation 2.3 and combining with equation 2.2, the unforced transfer function may be written:

$$Z_s/F_b = 1/(ms^2) \qquad 2.4$$

Its frequency response is shown in Figure 2.2.

The synchronous response problem occurs when the center of mass does not coincide with the geometric center. This is shown in block diagram form in Figure 2.3. This representation assumes that the position measured by the bearing is the rotor center of rotation. This resembles a disturbance rejection problem where Z_m is desired for measurement but only Z_s is available; however, the disturbance term is well understood. The disturbance magnitude is equal to the imbalance distance (ϵ) and the disturbance frequency is equal to the rotational speed (Ω),

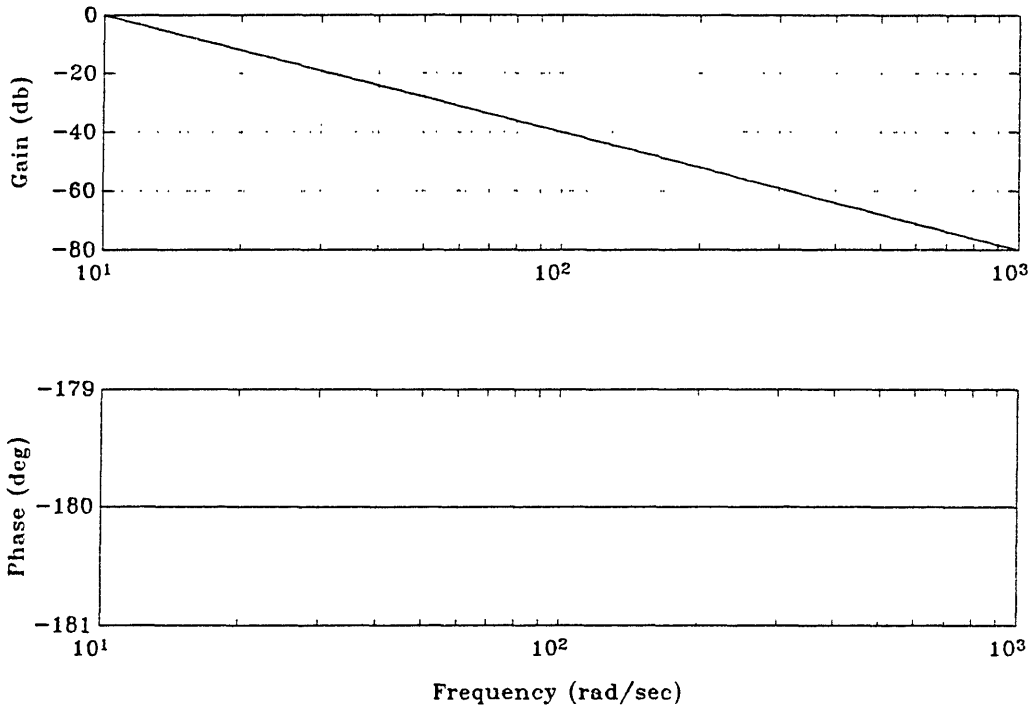

Figure 2.2. Rigid Rotor Frequency Response (Z_S/F_b)

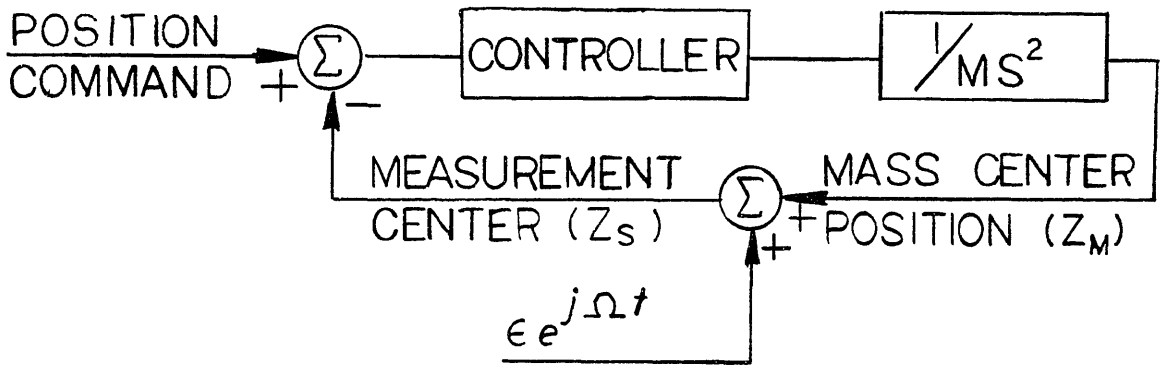

Figure 2.3. Block Diagram of Rigid Rotor with Mass Imbalance

hence the name synchronous disturbance.

The assumption of a rigid shaft is a good one for cases in which the shaft stiffness is much greater than the bearing stiffness, however, rotor systems are frequently designed with the bearings stiffer than the shaft. In these cases, a flexible rotor model is necessary.

2.2. Jeffcott Flexible Rotor Model

The Jeffcott rotor model consists of a centrally located unbalanced disk attached to a massless elastic shaft with spring constant k_s. This model was chosen because of its simplicity and its widespread use in describing the dynamics of flexible rotors [Jeffcott 1919]. The Jeffcott model figures prominently in Gunter's survey of work in the field of rotor dynamics [Gunter 1966] and is used throughout Johnson's thesis on the control of flexible rotors using magnetic bearings [Johnson 1985]. The history of modeling the flexible rotor and the evolution of the Jeffcott model are not given here but are well outlined by Gunter [1966] and Johnson [1985].

Figure 2.4 illustrates the geometry of the Jeffcott model. The elastic restoring force due to shaft bending is modelled as acting along an axis central to the shaft and will be referred to as the shaft elastic axis. The plane of the rotor intersects the shaft elastic axis at point S, which is offset from the rotor center of mass, M, by a distance ϵ_r. The intersection of the shaft elastic axis and the plane of the bearing is named the bearing center. Its projection onto the plane of the rotor is labelled point B. The shaft deflection, δ, is the distance between points B and S.

Figure 2.5 shows a projection of the geometry of Figure 2.4 onto the x-y plane. For simplicity, the origin is defined as the bearing center (B).

The Jeffcott model can predict several phenomena of flexible rotors including synchronous and asynchronous

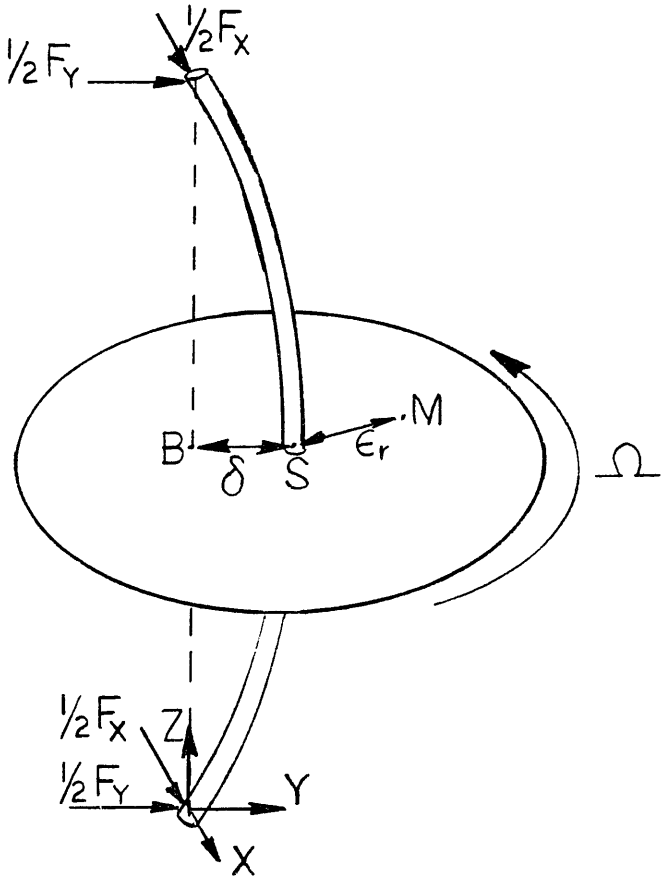

Figure 2.4. Jeffcott Rotor Model Geometry

vibrations, depending on the assumptions made in formulating the problem. An assumption which will be made in this paper is that the rotor precesses with the same angular velocity as its rotational speed, Ω. This behavior is called "synchronous precession". In other words, the plane of shaft flexure (containing line SB in Figure 2.4) rotates at the same angular velocity as the line between the rotor center of mass and the point connecting the shaft flexible axis to the rotor (line MS). The lines are offset in phase by the angle β. Assuming rigid bearings, an expression can be derived for the synchronous rotor deflection, δ, due to mass imbalance and is given by

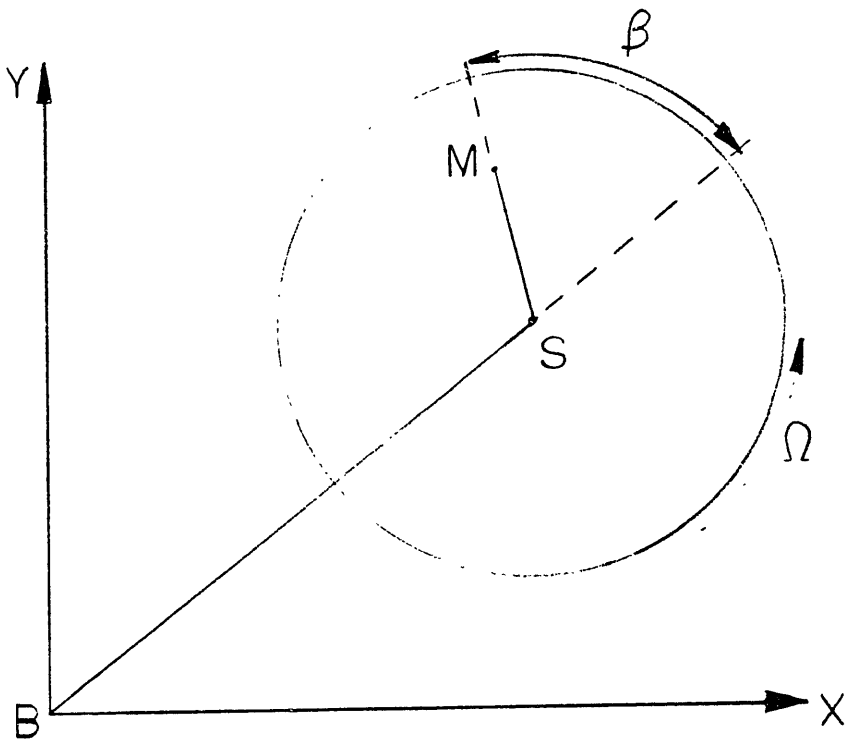

Figure 2.5. Planar Projection of Jeffcott Rotor Geometry

[Gunter 1966]:

$$\delta = \frac{\epsilon_r}{\sqrt{((\omega_s/\Omega)^2 - 1)^2 - (c_s/m\Omega)^2}} \qquad 2.5$$

where

δ = deflection of the shaft

ϵ_r = mass imbalance distance

ω_s = natural bending frequency of the shaft-rotor system

Ω = rotational speed

c_s = internal damping of the rotor

m = rotor mass

This function is shown in Figure 2.6, a graph of normalized rotor deflection versus normalized rotational speed. For low levels of damping, the rotor deflection becomes very large at ω_s, widely referred to as a rotor

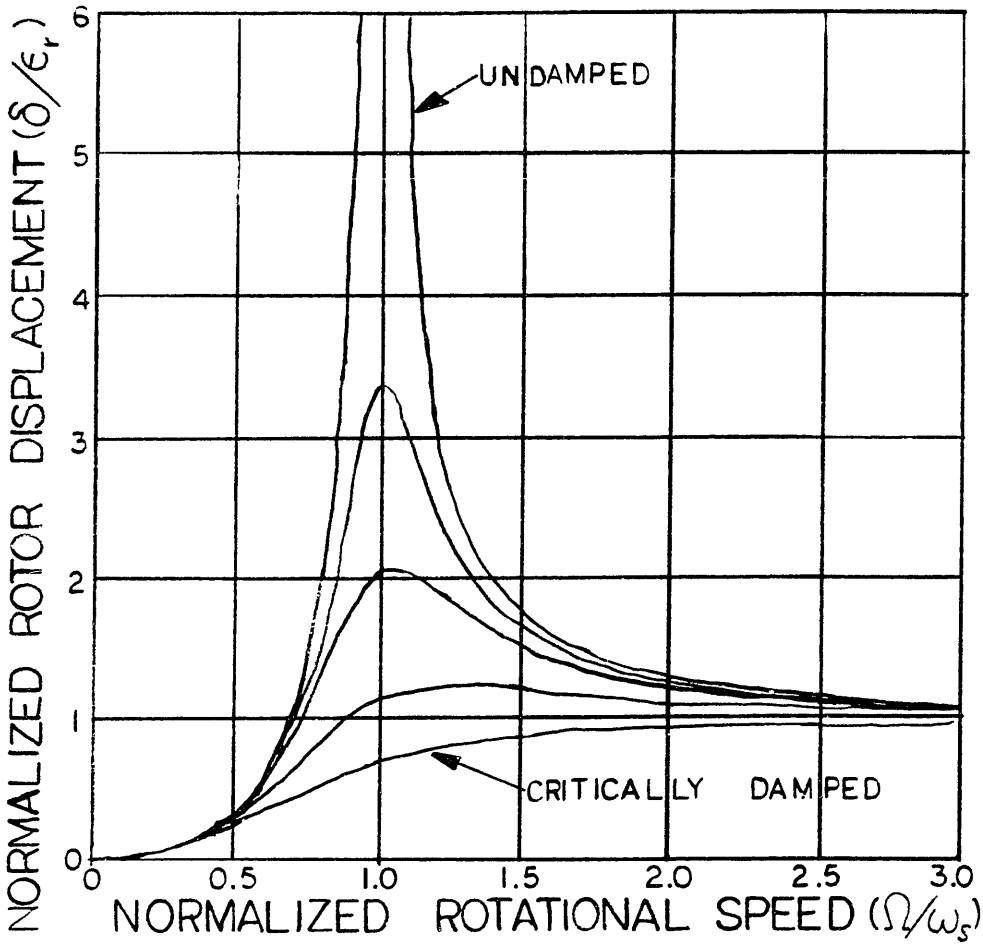

Figure 2.6. Rotor Deflection versus Rotational Speed

critical frequency. Since the rotor deflection at this frequency is due to shaft bending, it will be referred to as the rotor flexible frequency in this thesis, so as not to be confused with the critical frequency due to bearing flexibility. At higher rotational speeds, the rotor deflection approaches the imbalance distance (ϵ_r). The phase angle (β) also changes with rotational speed and is given by [Gunter 1966]:

$$\beta = \arctan\left[\frac{c_s/m\Omega}{(\omega_s/\Omega)^2 - 1}\right] \qquad 2.6$$

This relation is shown in Figure 2.7. At low rotational speeds the rotor center of mass (M) is nearly in phase with

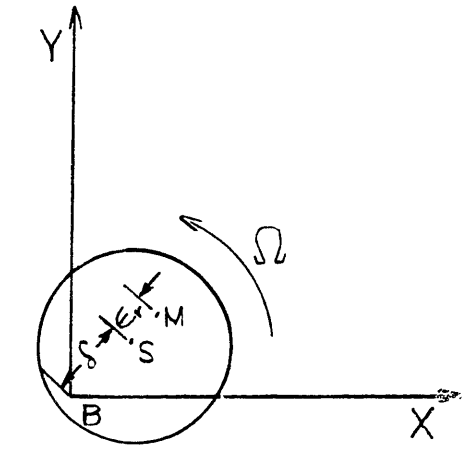

$\Omega << \omega_s, \beta = 0$

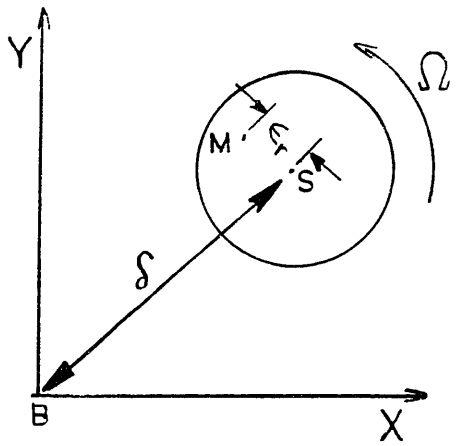

$\Omega = \omega_s, \beta = \frac{\pi}{2}$

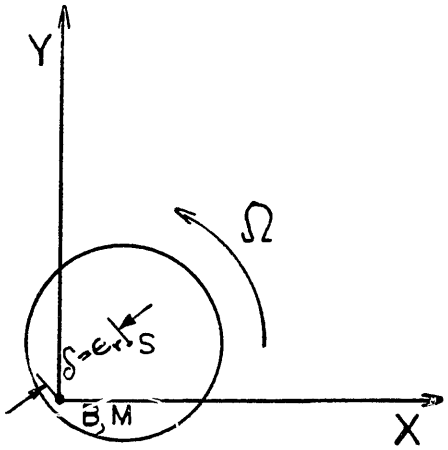

$\Omega >> \omega_s, \beta = \pi$

Figure 2.7. Phase Angle between Mass and Rotational Centers versus Rotational Speed

the rotor centerline SB. Near the rotor flexible frequency (ω_s), the center of mass leads the rotor centerline by 90 degrees and very large shaft deflections are observed. At high speeds, the center of mass is 180 degrees out of phase with the rotor centerline and the deflection is the mass imbalance distance (ϵ_r). The result is that the center of mass is stationary and coincident with point B as point S rotates about the mass center. To summarize, at low speeds the center of rotation is the rotor elastic (in this case geometric) center (S), requiring the center of mass (M) to spin about S. At high speeds, the center of rotation becomes the center of mass. In these conditions, the geometric center must spin about M.

The following pages present a brief derivation of the equations of motion of the Jeffcott rotor model assuming no shaft internal damping and an unspecified bearing force. Shaft internal damping is neglected here since it leads to asynchronous precession or rotor whirl, a phenomenon not addressed in this paper. The coordinate system used is shown in Figure 2.8, a planar projection of the Jeffcott shaft and rotor. This model assumes mass imbalance

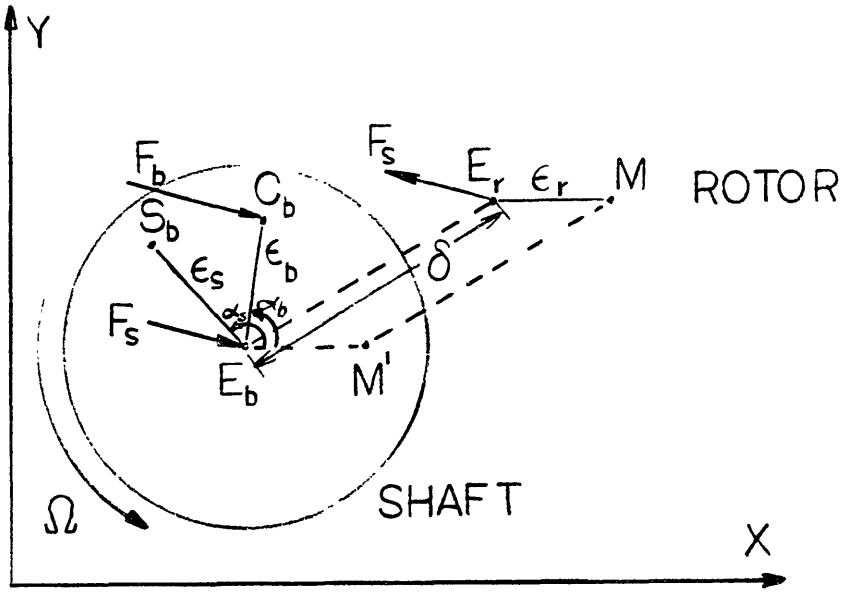

Figure 2.8. Planar Projection of Jeffcott Coordinate System

distance ϵ_r between the rotor center of mass (M) and the intersection of the elastic axis with the plane of the rotor (E_r). It is further assumed that the shaft elastic center at the bearing (E_b) is offset from the center of bearing force (C_b) by a distance ϵ_b and a phase angle α_b relative to the mass-imbalance distance (shown projected onto the plane of the bearing). Similarly, the center of bearing measurement (S_b) is offset from E_b by distance ϵ_s and phase angle α_s.

In describing the positions of the various points with respect to each other, it becomes expedient to use complex coordinates. Application of Newton's second law to the rotor gives a relation between the shaft force on the rotor and the position of the center of mass:

$$Z_m = F_s/(ms^2) \qquad 2.7$$

Since the shaft is assumed massless, Hooke's law applied to the shaft gives:

$$F_s = k_s(Z_{Eb} - Z_{Er}) \qquad 2.8$$

The result of misalignment between the shaft elastic axis (E_b) and the center of bearing force (C_b) is that the force applied by the bearing (F_b) causes torque fluctuations in the shaft. Since this misalignment causes no translational motion and the rotational dynamics of this model are ignored, point C_b does not enter into the equations of motion. It may be written that:

$$F_s = F_b. \qquad 2.9$$

Combining equations 2.3 and 2.5 gives:

$$Z_m = F_b/(ms^2). \qquad 2.10$$

This result is identical to the rigid rotor formulation, where bearing force is proportional to center of mass acceleration.

The difference between the two models lies in the position feedback parameter. Whereas the rigid rotor position feedback was simply the mass center with a synchronous disturbance, the flexible rotor model uses the bearing center of measurement (S_b) as a feedback. This is given as:

$$Z_{Sb} = Z_{Eb} + \epsilon_s e^{j(\Omega t + \alpha_s)} \qquad 2.11$$

Combining equations 2.4, 2.5 and 2.7 gives:

$$Z_{Sb} = F_b/k_s + Z_{Er} + \epsilon_s e^{j(\Omega t + \alpha_s)} \qquad 2.12$$

The position of the mass center (M) relative to the elastic center (E_r) is given as:

$$Z_m = Z_{Er} + \epsilon_r e^{j\Omega t} \qquad 2.13$$

Combining equations 2.8 and 2.9 gives:

$$Z_{Sb} = Z_m + F_b/(m\omega_s^2) + \epsilon_c e^{j\Omega t} \qquad 2.14$$

where:

$$\epsilon_c = \epsilon_s e^{j\alpha s} - \epsilon_r \qquad 2.15$$

The magnitude of ϵ_c, a complex number, does not represent a single distance, but is a combination of mass imbalance and measurement error distances.

The center of mass and center of measurement may be better understood when written in transfer function form. Equation 2.6 becomes:

$$Z_m/F_b = 1/(ms^2) \qquad 2.16$$

Combining equation 2.10 with equation 2.12 gives the unforced transfer function:

$$Z_{Sb}/F_b = (\omega_s{}^2+s^2)/(ms^2\omega_s{}^2) \qquad 2.17$$

The frequency response of equations 2.12 and 2.13 is given in Figure 2.9. The mass center behaves as a double integrator with phase of -180 degrees and gain decreasing with frequency by 40 db/decade. The bearing center has the same response as the mass center at frequencies below the shaft flexible frequency (ω_s). Above ω_s, the bearing center has a constant gain of $1/k_s$ and 0 phase.

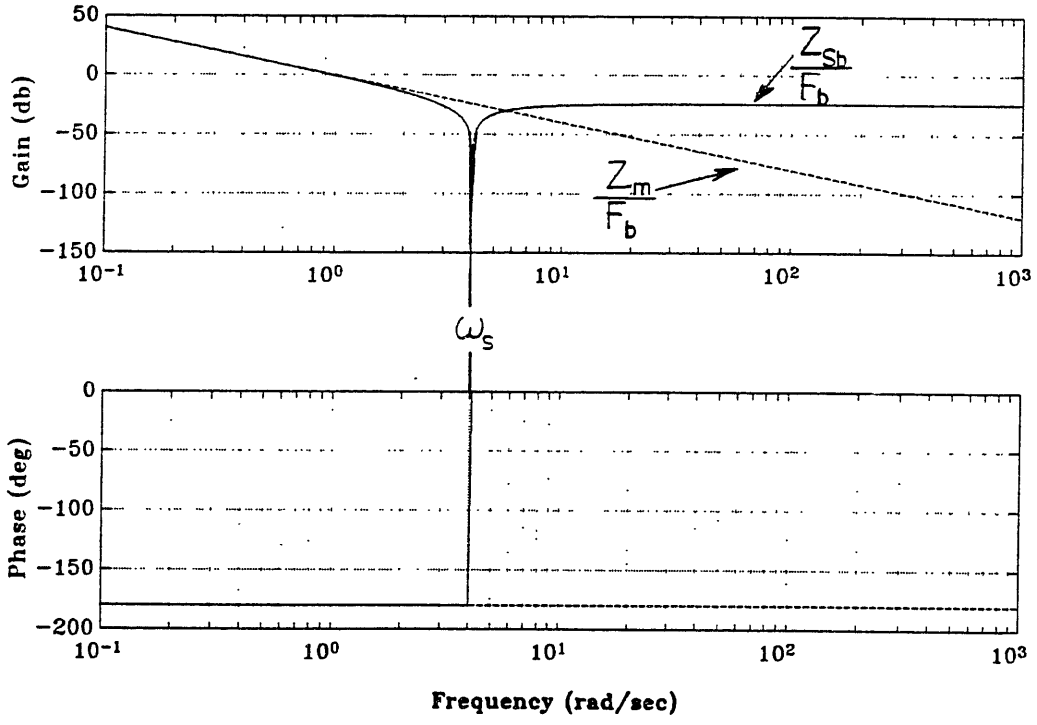

Figure 2.9. Flexible Rotor Synchronous Frequency Response (Z_{Sb}/F_b, Z_m/F_b)

In general, the transfer function of a rotor system is a function of both frequency and rotational speed, $G(s,\Omega)$. When studying synchronous behavior, the frequency of interest is the rotational frequency, therefore the frequency response is evaluated at this frequency, $G(s,\Omega)|_{s=j\Omega}$. This will be referred to as the synchronous frequency response because it is only a function of the rotational frequency. In this case however, the frequency response shown in Figure 2.9 is independent of rotational speed, therefore identical to the synchronous frequency response.

This analysis of the Jeffcott flexible rotor may be compared to Gunter's relations for deflection and phase in the following manner. The synchronous frequency response of the flexible rotor from bearing force (F_b) to mass center (Z_m) and bearing center (Z_{Sb}) is given in Figure 2.9. The shaft is essentially rigid below the flexible frequency; there is no shaft deflection ($\delta = 0$) and no difference in phase between mass and bearing centers ($\beta = 0$ degrees). This corresponds to rotation about the geometric axis. Above the flexible frequency, the two points are out of phase ($\beta = 180$ degrees). The synchronous frequency response also shows that at high rotational speed, bearing position is proportional to bearing force by a factor $1/k_S$. Since the bearing position is proportional to bearing force at high rotational speed, no centripetal force can be acting on the shaft because centripetal force is a function of speed-squared. In that case, the rotor must rotate about its mass center and the shaft deflection be equal to the combined imbalance distance (ϵ_C). The absence of shaft damping from this model causes an infinitely deep resonance to occur at the flexible frequency (ω_S). In other words, no amount of bearing force at ω_S can change the bearing position.

CHAPTER 3
CONVENTIONAL CONTROLLER DESIGN

To restate the ultimate objective of the controller, the bearings should not provide stiffness at the rotational frequency, thus allowing the rotor to spin about its inertial axis. This may be achieved by using a tracking notch filter to attenuate the position signal to the controller at the rotational speed.

First, it is necessary to design conventional control laws for the plants described in the previous chapter, i.e. controllers without notch filters. Once conventional controllers are designed, the stability characteristics and performance in rejecting the synchronous disturbance caused by mass imbalance can be used as a baseline in comparison to systems with tracking notch filters. The objective of this chapter is to define the requirements which the conventional controllers must meet and to show how each of them meets these requirements. The following chapter will discuss the characteristics of notch filters to give an idea of what changes the addition of a tracking notch filter will have on these conventional control systems.

The conventional control laws will need to meet general requirements, typical of actual magnetic bearing systems, and be sufficiently general so that the results can be easily applied to a variety of specific applications. Such requirements may include d.c. stiffness, crossover frequency, relative stability or damping, and disturbance rejection. The stability of the resulting system will be shown using Bode and Nyquist plots. The performance of the conventional control laws in rejecting the mass imbalance disturbance will be compared to the performance of the notch filter control laws in the chapters on notch filter controllers.

A proportional-integral-derivative (PID) control law was chosen for this study because it is simple to

implement, and as a result, widely used. For the system to meet the design requirements, proportional, integral or derivative control action may be selected for any range of frequencies. For instance, in bearing design, high d.c. stiffness is desirable to maintain rotor position under the influence of gravity and other low frequency disturbances. In that case, integral action would be called for at low frequencies to give high gain at low frequencies. Double integrator plants requires derivative control action around the crossover frequency to give the system phase margin, necessary for stability. Since differentiation over a wide frequency range is not physically realizable, the range of derivative action centered at the crossover frequency will be limited to one decade.

The bearing crossover frequency (ω_c) approximately represents the bandwidth of the bearing-rotor system, i.e. the control system responds to disturbances in rotor position below ω_c but not above it. The crossover frequency is determined, in the case of conventional ball or roller bearings, by the bearing stiffness and is usually chosen to be above the highest frequency of bearing position disturbance to which the rotor must respond. For conventional bearings, the d.c. stiffness is directly linked to the crossover frequency. In magnetic bearing systems, the crossover frequency is chosen based on the same criteria as conventional bearings but is determined by the system gain. Since the system gain may be made a function of frequency by PID control, the crossover frequency may be chosen independently of the d.c. gain.

3.1. Rigid Rotor Controller

The requirements of the rigid rotor controller, as outlined above, are stability and some crossover frequency which is typical of an actual magnetic bearing system. The loop gain and phase is shown in Figure 3.1. A double integrator plant, as in this case, may be controlled by

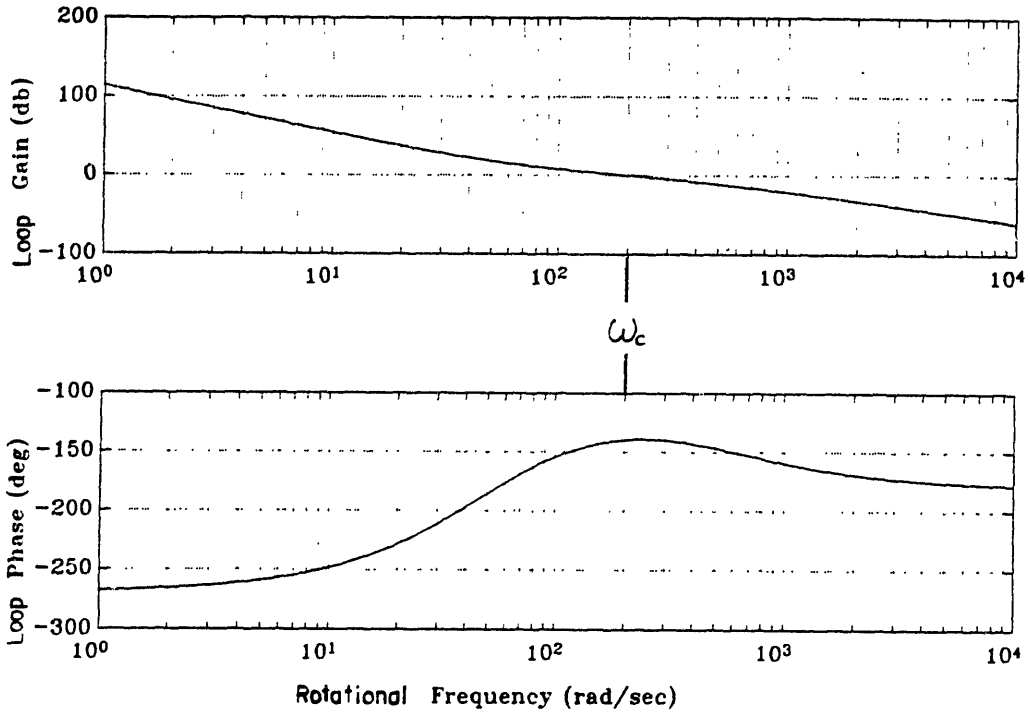

Figure 3.1. Loop Frequency Response, Rigid Rotor System

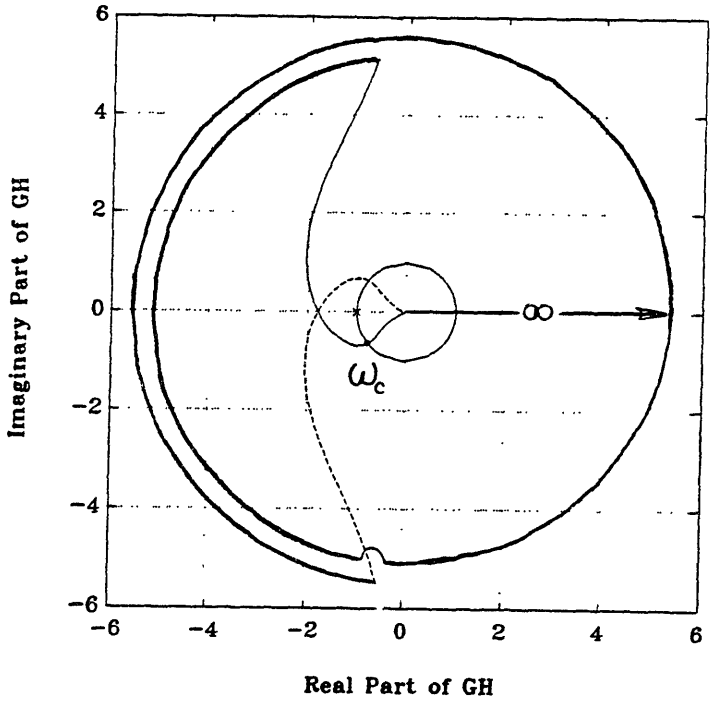

Figure 3.2.Loop Nyquist Plot, Rigid Rotor System

lead-lag compensation or derivative action centered at the crossover frequency. Note that the extent of derivative action determines the amount of phase margin, hence the system relative stability. Low frequency integral action helps raise the low frequency gain without affecting the system stability significantly.

Polar plots can also be used to represent the open loop frequency response graphically. An advantage of polar plots over Bode plots is that the magnitude and phase information is condensed into one graph. This advantage will prove especially useful in the stability analysis of the system with the notch filter included. As a grounds for later comparison, a Nyquist plot of the present system is given in Figure 3.2 on modified logarithmic axes. The axes are modified to condense information closer to the origin without changing the location of the unit circle. Therefore this plot may still be used to determine system stability by observing the total number of encirclements of the point (-1 + 0j). A brief background of the Nyquist stability criterion and justification for the modified axes used here are given in Appendix A.

The modified Nyquist plot of this system consists of the open loop transfer function plotted on the real and imaginary axes. The part of the curve corresponding to negative frequencies is simply the reflection about the real axis of the curve for positive frequencies and is given as a dotted line. The number of open loop poles at the origin determines the number of semicircles at infinity, in this case three. Since the systems to be studied have no zeroes in the right half s plane, the number of counterclockwise encirclements of the point (-1 + 0j) corresponds to the number of open loop poles in the right half s plane. The number of encirclements of the point (-1 + 0j) may be found by following the curve in the direction of increasing frequency, starting at zero. By this method, it is apparent that the rigid rotor and

controller are stable.

This system's performance in rejecting the synchronous mass imbalance disturbance can be found by taking the closed loop frequency response from synchronous mass imbalance disturbance ($\epsilon e^{j\Omega t}$) to the center of mass position (Z_m) and ignoring the position command input. The notation here refers to Figure 2.3. The synchronous frequency response of the closed loop system is given in Figure 3.3. In this case, neither plant nor controller are functions of rotational speed (Ω), therefore the closed loop frequency response is identical to the synchronous frequency response. It shows that the system does not

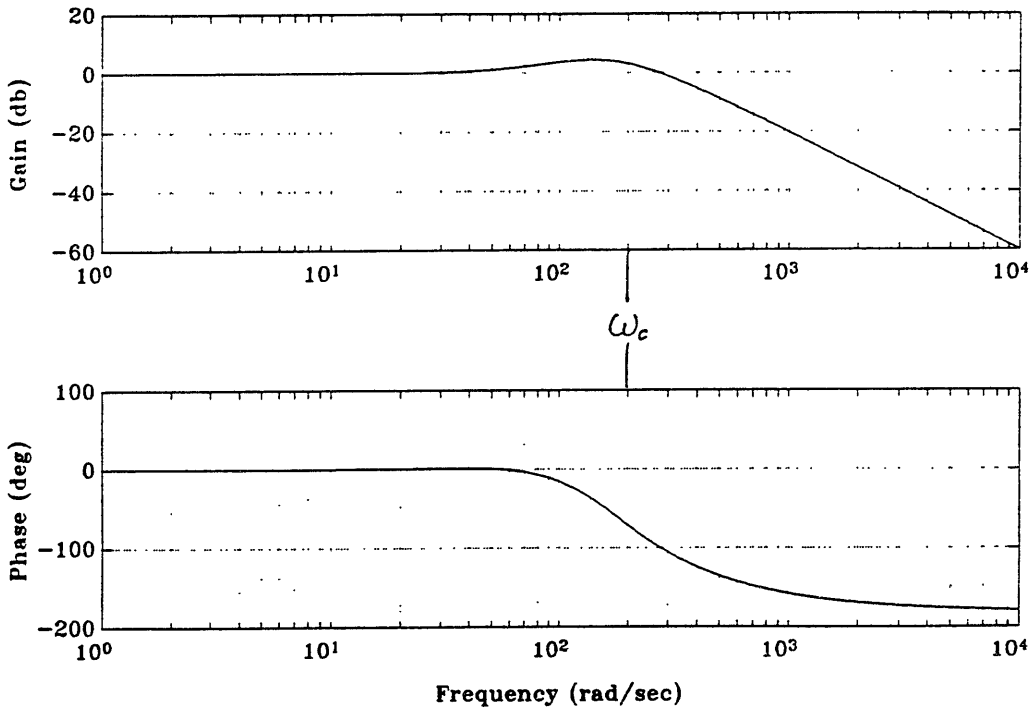

Figure 3.3. Closed Loop Synchronous Frequency Response of Rigid Rotor System ($Z_m/\epsilon e^{j\Omega t}$)

reject the synchronous mass imbalance disturbance below the crossover frequency (ω_c). Above ω_c, the closed loop frequency response resembles that of the open loop system; the gain decreases at 40 db/decade. The synchronous mass imbalance disturbance is increasingly attenuated with increasing rotational speed above the crossover frequency. In other words, when the system gain is below unity, the bearing stiffness is insufficient to maintain the air gap constant in response to the synchronous forcing function caused by the mass imbalance. As a result, the rotational axis gradually migrates from the geometric axis to the inertial axis.

3.2. Flexible Rotor Controller

Control of the flexible rotor plant is unique because there are two distinct outputs which may be fed back. A block diagram of the plant, shown in Figure 3.4, reveals that either bearing or rotor position may be used. The transfer function from bearing force to rotor center of mass position is given in equation 2.12 and the unforced transfer function between bearing force and bearing position is given in equation 2.13. The measured bearing position (Z_{Sb}) includes a complex imbalance distance (ϵ_c). Similarly, locating the position sensor at the rotor introduces measurement error and offsets the measured position (Z_S) from the actual center of mass (Z_m) by a distance (ϵ), using the same notation as for the rigid rotor model.

Feedback of the rotor position is not widely used because of the existence of "spillover effects". This term refers to phenomena in which the higher flexible modes of the rotor shaft are destabilized because the sensor and actuator are not "colocated", that is the position sensor is located at the rotor whereas the magnetic bearing acts at the bearing. This arrangement only controls the position of the rotor and does not account for shaft motion

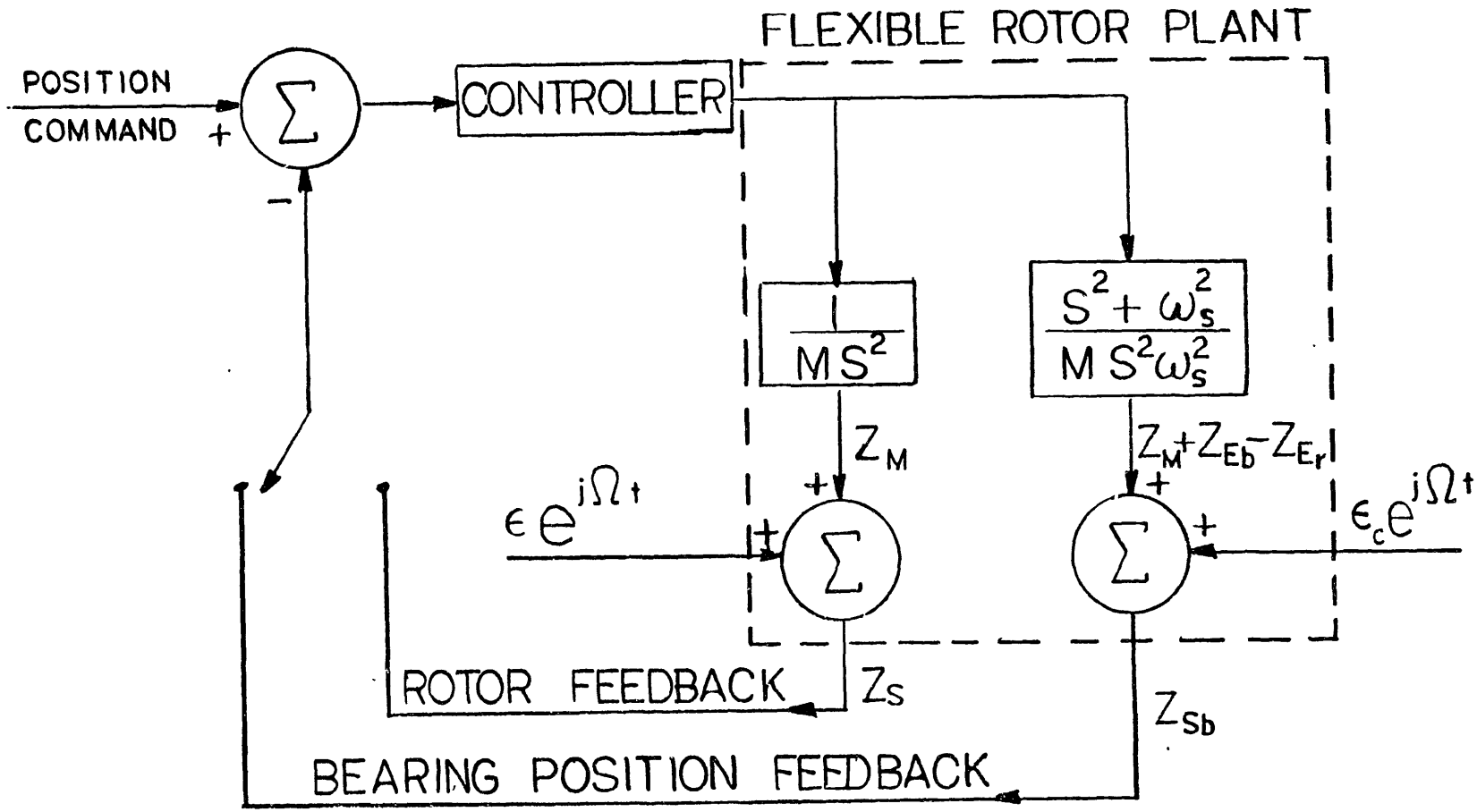

Figure 3.4. Block Diagram of Flexible Rotor Control Loop

due to higher vibrational modes. In this case, however, the shaft is assumed to be massless and therefore without higher modes. Initially, feedback of the bearing position, i.e. local feedback, will be discussed.

3.2.1. Bearing Feedback

The synchronous frequency response of the plant is given in Figure 2.9. Since this controller will use bearing position for feedback, the stability analysis should use the transfer function from bearing force (F_b) to bearing position (Z_{Sb}). The frequency response shows that an infinitely deep resonance exists at the shaft flexible frequency (ω_s). At frequencies below ω_s, the rotor mass dominates the dynamics since the shaft is essentially rigid at low frequencies. At frequencies above ω_s, the bearing force goes primarily to bending the shaft rather than moving the rotor mass. Consequently, the gain at high frequency is constant and equal to the shaft compliance ($1/k_s$).

Design of the control law for the flexible rotor requires an approach similar to that used in the design of the rigid rotor controller. Stability is provided by derivative action and the crossover frequency is chosen to meet the desired requirements. The crossover frequency (ω_c) is determined by the bearing stiffness, or controller gain, and may be chosen to be either above or below the shaft flexible frequency (ω_s). These two cases will be addressed separately since they call for different controller designs. A system with the bearing crossover frequency (ω_c) greater than the shaft flexible frequency (ω_s) physically represents the shaft relatively soft, or flexible, compared to the bearings. Conversely, when the crossover frequency is less than ω_s, the bearings are soft relative to the shaft.

3.2.1.1. Stiff Shaft/Soft Bearings

The loop gain and phase of a system with a stiff shaft relative to the bearings and bearing feedback is shown in Figure 3.5. This system may be stabilized using the same control as for the rigid rotor model because the resonance at ω_s occurs above the crossover frequency (ω_c) and can have no influence on system stability. Integral control action at low frequency gives high gain and a loop phase of -270 degrees at low frequency. One decade of derivative action at ω_c increases phase, giving phase margin as before. In this case, it may be desirable to include integral action at high frequency as well, to enhance rejection of high frequency noise by reducing the gain. However, this was omitted since it is peripheral to the study of the tracking notch filter.

The design of this control law is justified by referring to the Nyquist plot shown in Figure 3.6. The effect of the resonance is limited to the interior of the unit circle, thus preventing the resonance from causing any encirclements of the point (-1 + 0j). This result justifies the use of the same controller for the "stiff shaft" model as for the rigid rotor model. This makes sense intuitively since the rigid rotor model is just a degenerate case of the stiff shaft model.

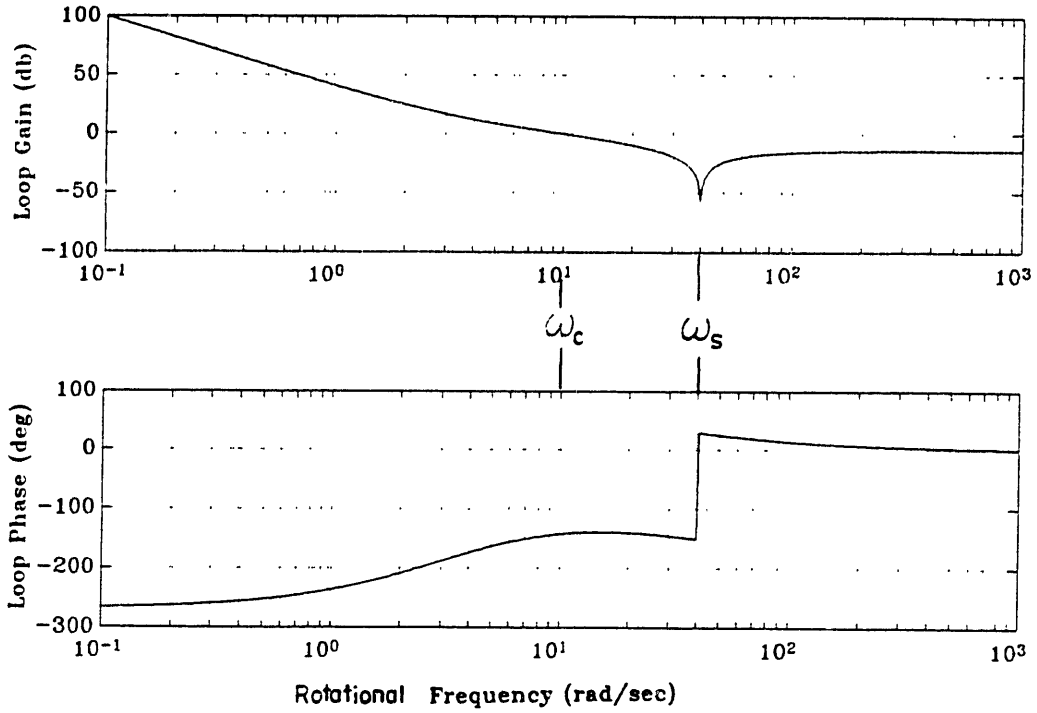

Figure 3.5. Loop Frequency Response, Flexible Rotor (Bearing Feedback, Stiff Shaft) System

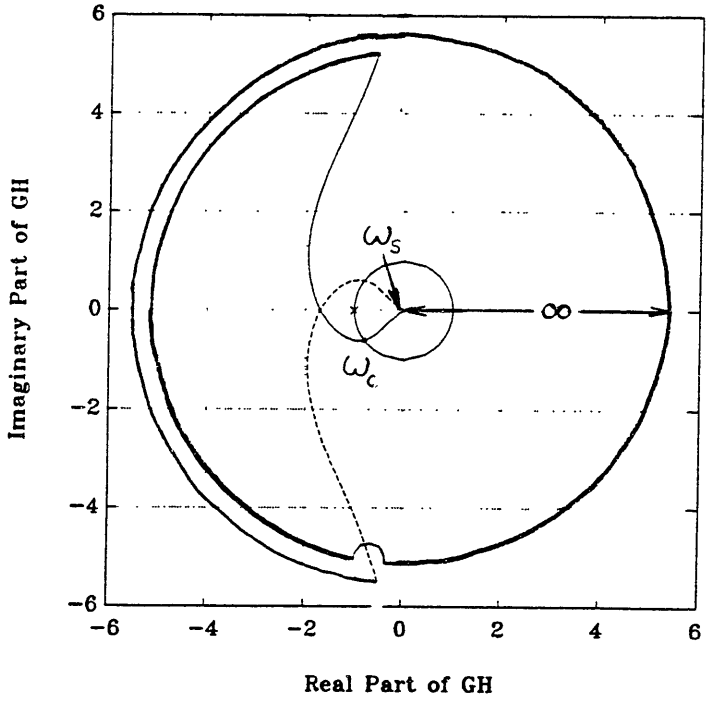

Figure 3.6. Loop Nyquist Plot, Flexible Rotor (Bearing Feedback, Stiff Shaft) System

3.2.1.2. Soft Shaft/Stiff Bearings

A system with a soft shaft relative to the bearings imposes new requirements on the controller design. The loop gain and phase of such a system are shown in Figure 3.7. The control law must allow the bearings to respond in two regimes; when the shaft is essentially rigid, at speeds below the flexible frequency (ω_s), and when shaft bending predominates, at speeds of ω_s and above.

To stabilize this plant, two actions must be taken. First, the plant must be rolled off in a stable manner, i.e. using integral control action at high frequency. This makes the loop phase -90 degrees at the crossover frequency. Secondly, since loop phase just below the flexible frequency (ω_s) is -180 degrees, one decade of derivative control action is added to give phase margin and a stable crossover at this frequency. Although integral control action was used at low frequency for the rigid rotor and the stiff shaft plants, it will be omitted from this controller since it does not significantly affect the synchronous response characteristics, as will later be shown. This results in a loop phase at low frequency of negative 180 degrees. It is also desirable to show that integral action at low frequency is not necessary for stability.

Using only phase and gain margins from the open loop synchronous frequency response, shown in Figure 3.7, to determine the system stability is tricky because of the existence of multiple crossovers (at ω_s and ω_c) and a sudden shift in phase near the shaft flexible frequency (ω_s).

In this case, the stability is easier to quantify using the Nyquist plot, shown in Figure 3.8. Without integral control action at low frequency, the Nyquist curve now approaches the origin from the negative real axis. The resonance causes the curve to pass through the origin and to the other side, representing zero gain at ω_s and a shift

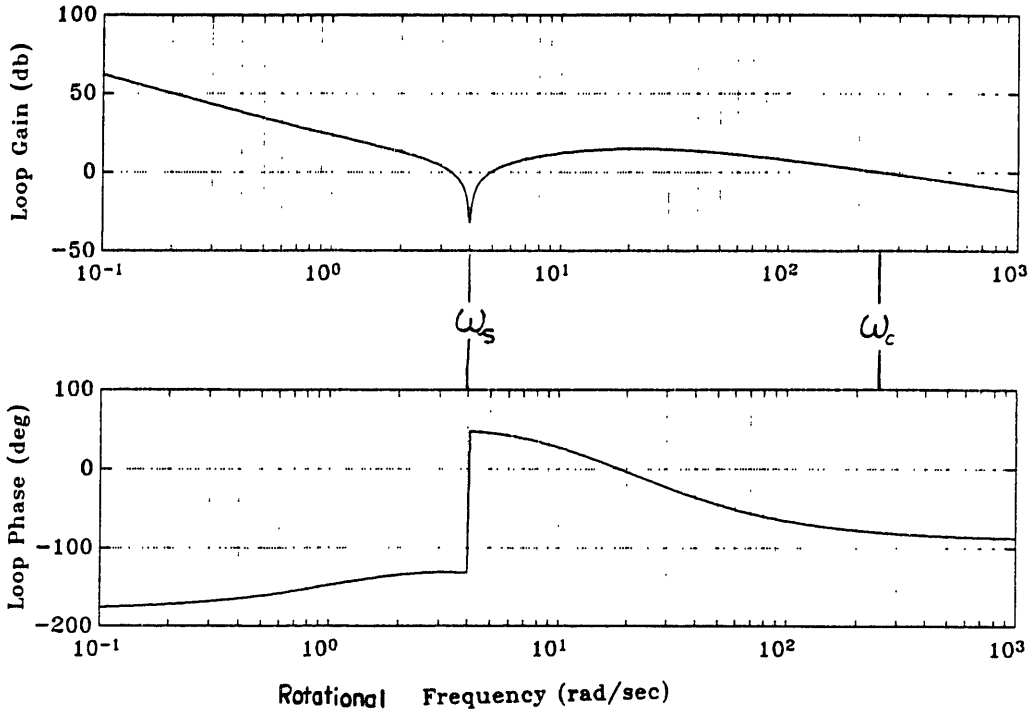

Figure 3.7. Loop Frequency Response, Flexible Rotor (Bearing Feedback, Soft Shaft) System

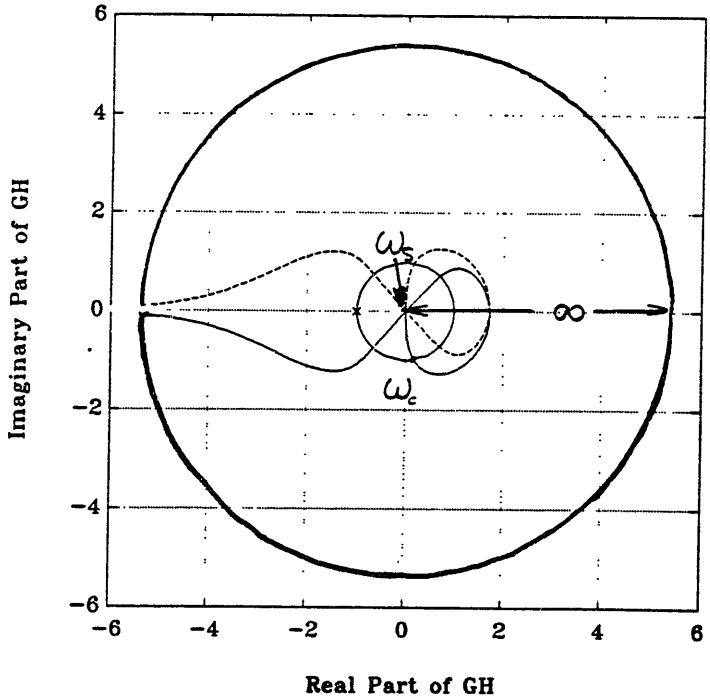

Figure 3.8. Loop Nyquist Plot, Flexible Rotor (Bearing Feedback, Soft Shaft) System

in phase of 180 degrees. Derivative action at ω_c acts to deflect the curve below the point (-1 + 0j) by adding phase in this area. High frequency integral action causes the curve to enter the origin with a phase of -90 degrees. The two poles at the origin of the s plane map to one encirclement of the origin at infinite radius. The total number of encirclements of the point (-1 + 0j) is zero, resulting in a stable system.

3.2.2. Rotor Feedback

By measuring rotor position directly, the flexibility of the shaft is not observed by the controller. Since this plant shares the same transfer function as the rigid rotor model, the same controller can be used for both [Johnson 1985]. For simplicity, this controller will omit low frequency integral action. Derivative action at the crossover frequency stabilizes the system as before. The system loop gain and phase show good stability, as seen in Figure 3.9. This is corroborated by the Nyquist plot, shown in Figure 3.10. Once again, the causes of spillover are not included in this model of rotor position feedback.

To review, the control laws derived in this chapter are sufficient to control the magnetic bearing systems for which each was designed. Each system meets requirements such as bearing crossover frequency, stability, d.c. gain and has some level of performance in rejecting the synchronous disturbance due to mass imbalance. From Figure 3.3, it appears that the synchronous disturbance is only rejected above the crossover frequency and increasingly so with increasing frequency. Thus, there is a trade-off between crossover frequency location and synchronous disturbance rejection. Performance of these systems in rejecting the synchronous mass imbalance disturbance will be discussed further in the chapter on notch filter controllers.

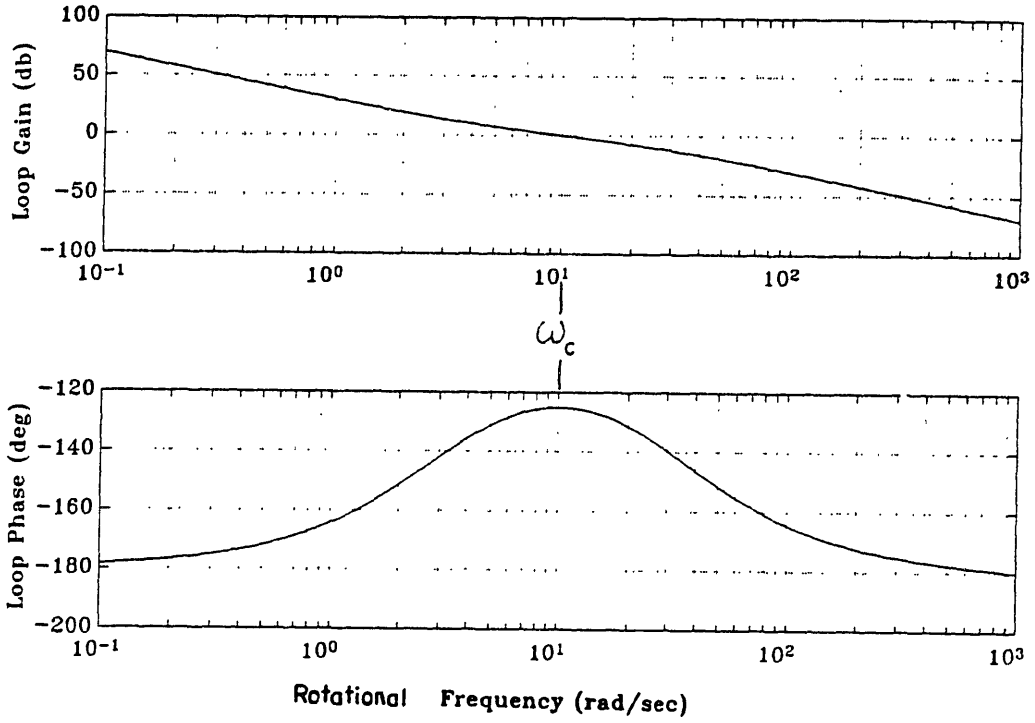

Figure 3.9. Loop Frequency Response, Flexible Rotor (Rotor Feedback) System

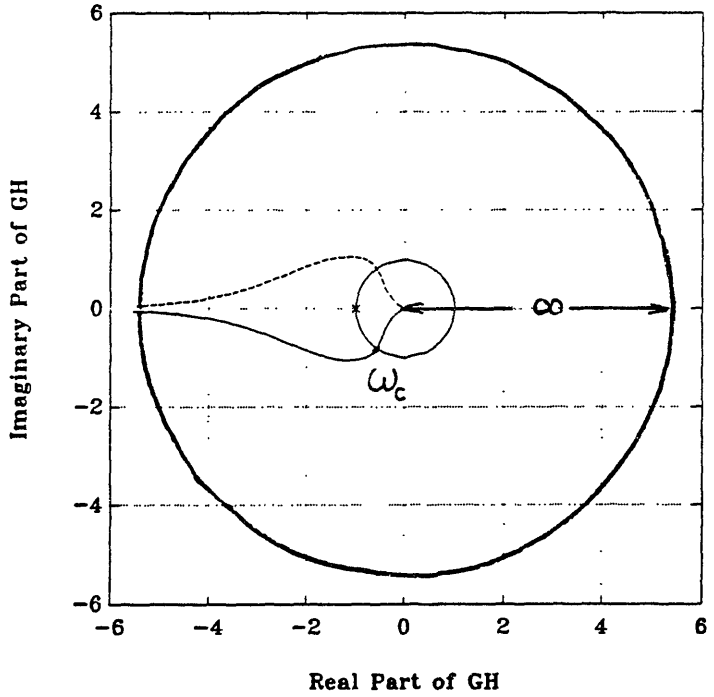

Figure 3.10. Loop Nyquist Plot, Flexible Rotor (Rotor Feedback, Soft Shaft) System

CHAPTER 4
NOTCH FILTER CHARACTERISTICS

An alternate means of increasing the performance, as previously discussed, is by the addition to the control law of the tracking notch filter at the rotational speed. This chapter gives a brief description of the capabilities and characteristics of notch filters. A notation is provided here which will be used throughout the following chapters, where the addition of the notch filter to the control loop will be examined.

A notch filter is a band-reject filter which attenuates over a very narrow frequency range. It is generally used to reduce the amplitude of a signal at a specific frequency. Notch filters are typically implemented by the ratio of two resonant structures. The particular notch filter design used here is the ratio of two second order polynomials. This may be represented dynamically as;

$$G_n(s) = \frac{s^2 + 2\xi_n\omega_o s + \omega_o^2}{s^2 + 2\xi_d\omega_o s + \omega_o^2} \qquad 4.1$$

where ξ_n and ξ_d represent damping coefficients and ω_o is the center frequency of the notch. A particular notch filter design can be characterized by its depth at ω_o and the Q factor, representing the steepness with which the gain drops off near ω_o.

The notch gain at ω_o is simply the ratio of the two damping terms;

$$D = G_n(j\omega_o) = \xi_n/\xi_d \qquad 4.2$$

The depth of the notch is typically chosen depending on the desired amount of attenuation at ω_o. From equation 4.2, a notch with infinite attenuation (zero gain at ω_o) must be designed with zero damping in the numerator. This places

two zeroes on the imaginary axis of the s plane. The frequency response of notch filters with varying depths and a constant value of Q are shown in Figure 4.1. An apparent trend is that the maximum variation in phase near ω_o increases with increasing notch depth, approaching a maximum variation of 180 degrees for a notch of infinite depth.

In designing a notch, the notch steepness is determined based on the distribution of the signal to be attenuated around ω_o. If the signal contains frequency components over a relatively wide range, a broad notch may be chosen in order to attenuate at ω_o as well as its neighboring frequencies.

The notch steepness is indicated by the parameter Q, where;

$$Q = \frac{1}{2\xi_d} = \frac{\omega_o}{\omega_2 - \omega_1} \qquad 4.3$$

and where ω_1 and ω_2 are the frequencies where the magnitude response is -3 dB [Huelsman, 1971]. The greater the value of Q, the steeper the drop in gain near the center frequency. Figure 4.2 shows the frequency response of notches with varying values of Q at a constant depth. The maximum amount of phase shift is independent of Q, whereas the abruptness of the phase change increases with Q.

Tracking notch filters have the advantage that they are not limited to a constant center frequency. They are capable of attenuating over a frequency range which varies with time. The filter receives the desired center frequency as an input and tracks it. This is particularly useful in attenuating the synchronous disturbance, since it occurs at the rotational frequency of the shaft. The transfer function of the notch filter which tracks rotational speed (Ω) becomes:

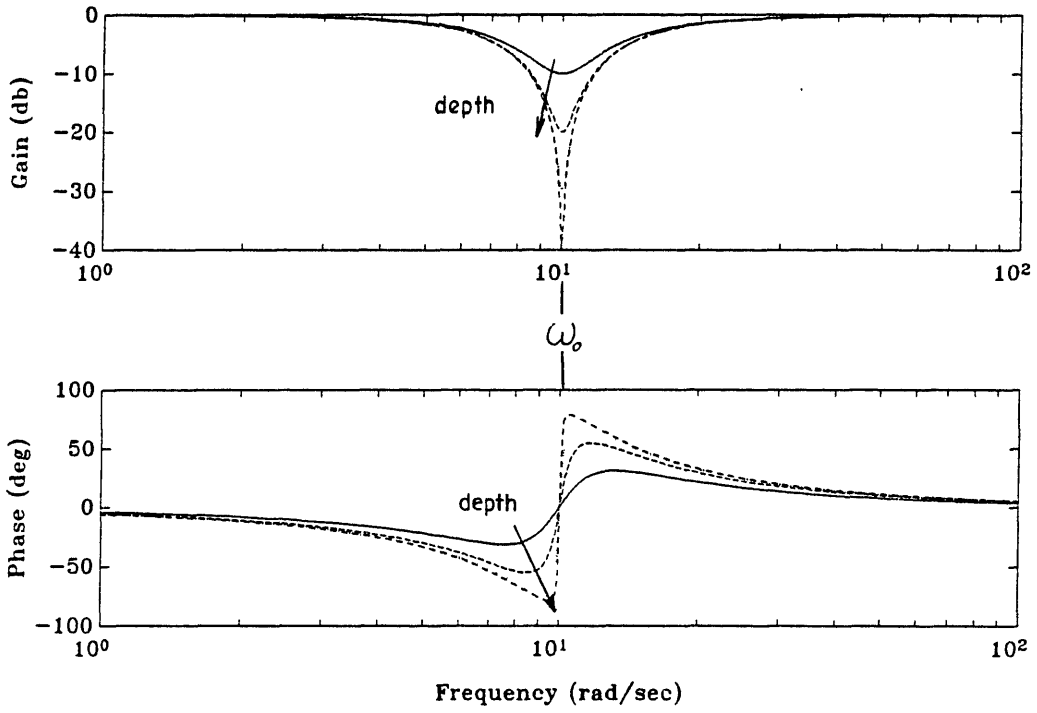

Figure 4.1. Notch Filter Frequency Response, Depth Varied, Constant Q Factor (Q = 1)

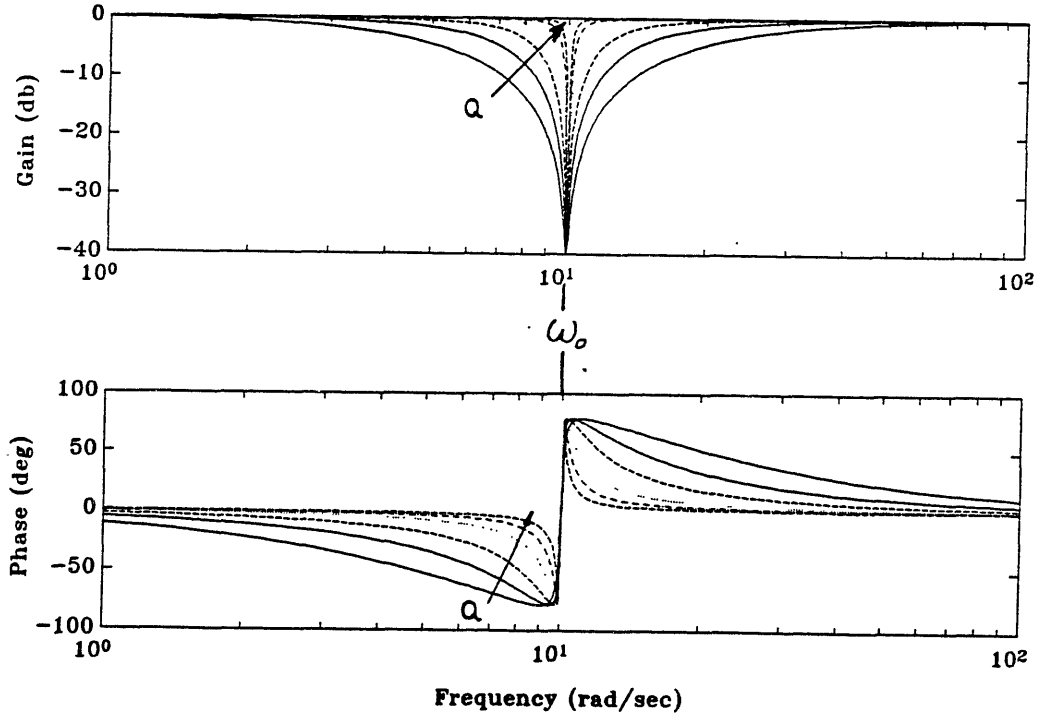

Figure 4.2. Notch Filter Frequency Response, Q Factor Varied, Constant Depth (40db)

$$G_n(s,\Omega) = \frac{s^2 + 2\xi_n\Omega s + \Omega^2}{s^2 + 2\xi_d\Omega s + \Omega^2} \qquad 4.4$$

A block diagram of the system with the addition of the tracking notch filter is shown in Figure 1.4. With the addition of the notch filter, the loop transfer function of this system becomes dependant on rotational speed. With this dependance on rotational speed, the term synchronous frequency response takes on a distinct meaning.

CHAPTER 5
NOTCH FILTER CONTROLLER STABILITY

This chapter will first explore the stability limitations imposed by the addition of the tracking notch filter to the control loop. For each of the control systems discussed so far, the unstable speed ranges will be defined and any dependence on notch filter design such as depth (D) and steepness (Q) will be discussed. Once stable operating regions have been defined, the following chapter will discuss the improvement in performance (rejection of the synchronous mass imbalance disturbance) caused by the notch filter over a range of rotational frequencies.

The addition to the control loop of the tracking notch filter, having a transfer function dependent on rotational frequency, likewise gives the open loop system transfer function a dependence on rotational frequency. The loop gain and phase of the rigid rotor system with a notch filter is shown in Figure 5.1 for a rotational frequency of 10 radian/second. The loop gain is reduced by the notch depth (D) at the rotational frequency (Ω) and the loop phase is shifted near Ω according to the notch filter parameters Q and D (reference Figures 4.1 and 4.2). As discussed in Chapter 2, the synchronous frequency response is the frequency response evaluated at the rotational frequency, $G(s,\Omega)|_{s=j\Omega}$. The synchronous loop gain and phase of the system above are shown in Figure 5.2. The only effect the notch filter has is to reduce the synchronous loop gain uniformly by the notch depth, in this case 40 db. The synchronous loop phase is unaffected by the addition of the notch filter because the notch introduces no phase shift at the rotational frequency (Ω).

The phase shift introduced by the notch filter can destabilize the control loop over certain ranges of rotational frequency. Generally, instability is caused when the phase lost by the notch filter at a crossover

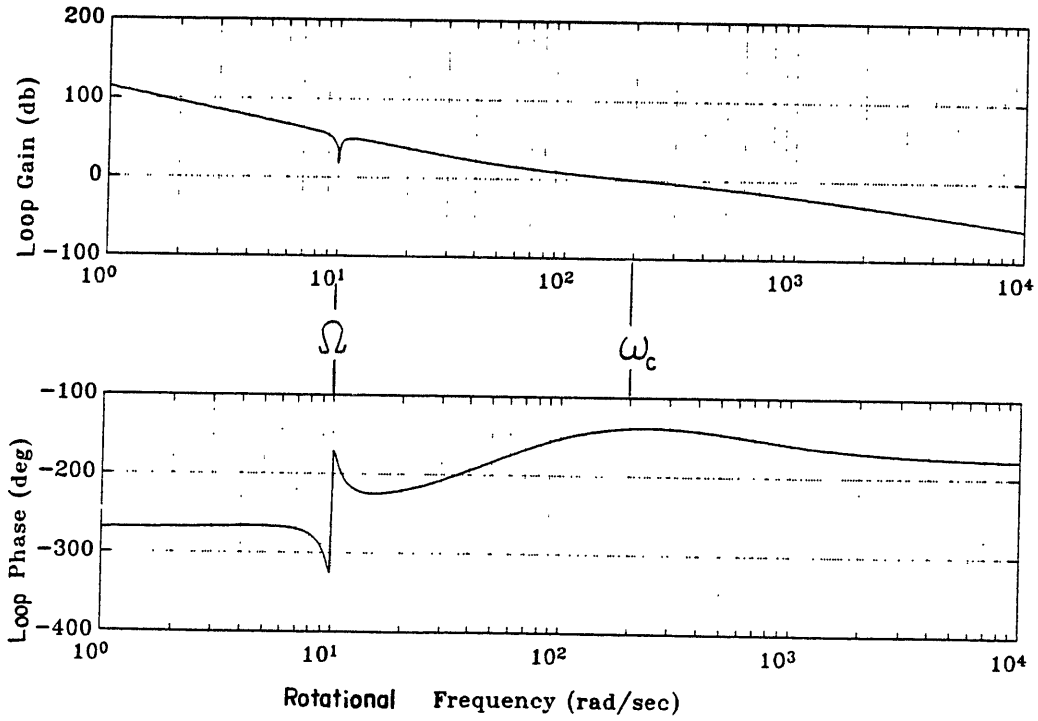

Figure 5.1. Loop Frequency Response, Rigid Rotor, Notch Filter Controller ($\Omega = .05\omega_c$)

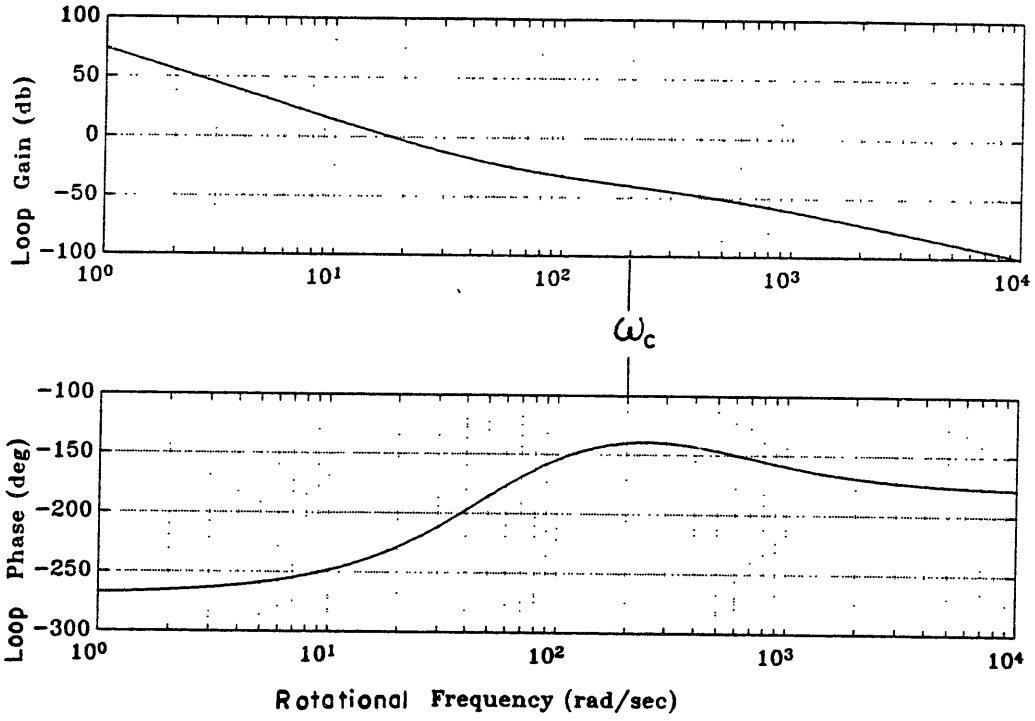

Figure 5.2. Synchronous Loop Frequency Response, Rigid Rotor, Notch Filter Controller

frequency exceeds the phase margin of the conventional control system. In other words, instability usually occurs when the loop phase of the system with the notch filter drops below -180 degrees at a system crossover frequency.

5.1. Rigid Rotor Control System

The bounds of the unstable speed range will be shown here to be a function of the notch parameters Q and D. Initially, a nominal notch filter design is chosen and the unstable speed range will be defined by examining the loop gain and phase and Nyquist plot with the nominal notch filter for a variety of different rotational frequencies (Ω). This nominal notch filter will have a depth of 40 db and Q factor of 5. Once the cause of instability is clarified, the effect of notch Q and depth (D) on the extent of the unstable speed range will be estimated.

The transition of the system from stable to unstable and back again is made clear by observing the system frequency response as the rotational frequency is gradually increased from a low value. Figure 5.1 shows the loop gain and phase of the rigid rotor system (reference Figure 3.1) with the nominal notch filter design at a rotational frequency chosen relative to the crossover frequency at $\Omega = .05\omega_c$. The notch filter causes roughly 90 degrees of additional phase loss at frequencies just below Ω, but since the notch depth is insufficient to drive the loop gain at Ω (synchronous loop gain) below unity, the system is stable. The Nyquist plot of this system is shown in Figure 5.3. Compared with the Nyquist plot of the rigid rotor system without the notch filter (reference Figure 3.2), it is apparent what the notch filter adds to the Nyquist curve. The notch pulls the curve toward the origin at the rotational frequency (Ω) and gives a wide phase shift in this vicinity; clockwise at frequencies below Ω and counterclockwise above Ω. The net result is no additional encirclements of the point (-1 + 0j), therefore

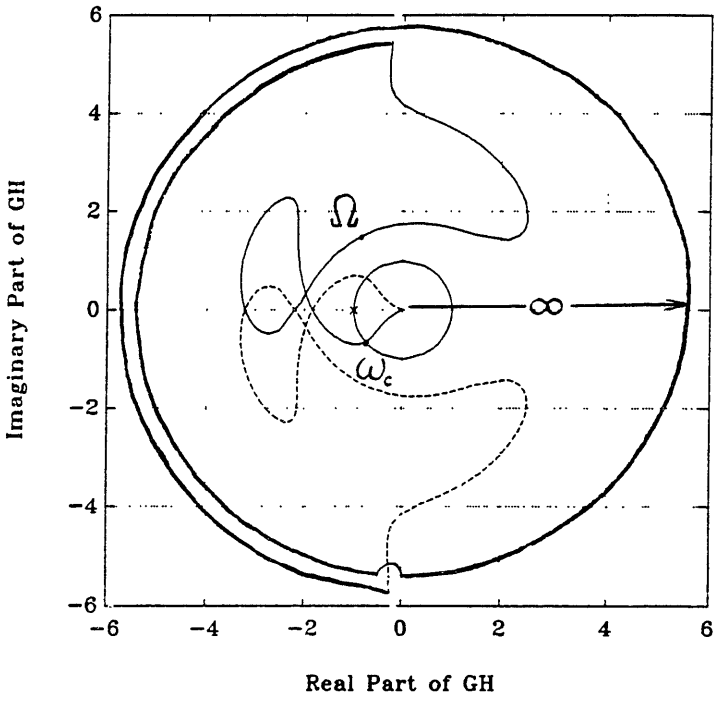

Figure 5.3. Loop Nyquist Plot, Rigid Rotor, Notch Filter Controller ($\Omega = .05\omega_c$)

a stable system.

The next case is when the rotational frequency is $\Omega = .1\omega_c$. This value of rotational frequency was chosen because the loop gain begins to dip below unity here, as shown in Figure 5.4. At the two crossover frequencies of loop gain near Ω, the loop phase is less than -180 degrees. This is more easily seen on the Nyquist plot of this system, shown in Figure 5.5. The notch filter causes the Nyquist curve to enter the unit circle at approximately negative 270 degrees and leave the unit circle at slightly less than -180 degrees. Since the curve did not pass to the inside of the point (-1 + 0j), the point has no additional encirclements and the system is still stable, but just barely so. Any further increase in the rotational frequency would reduce the phase at the crossover

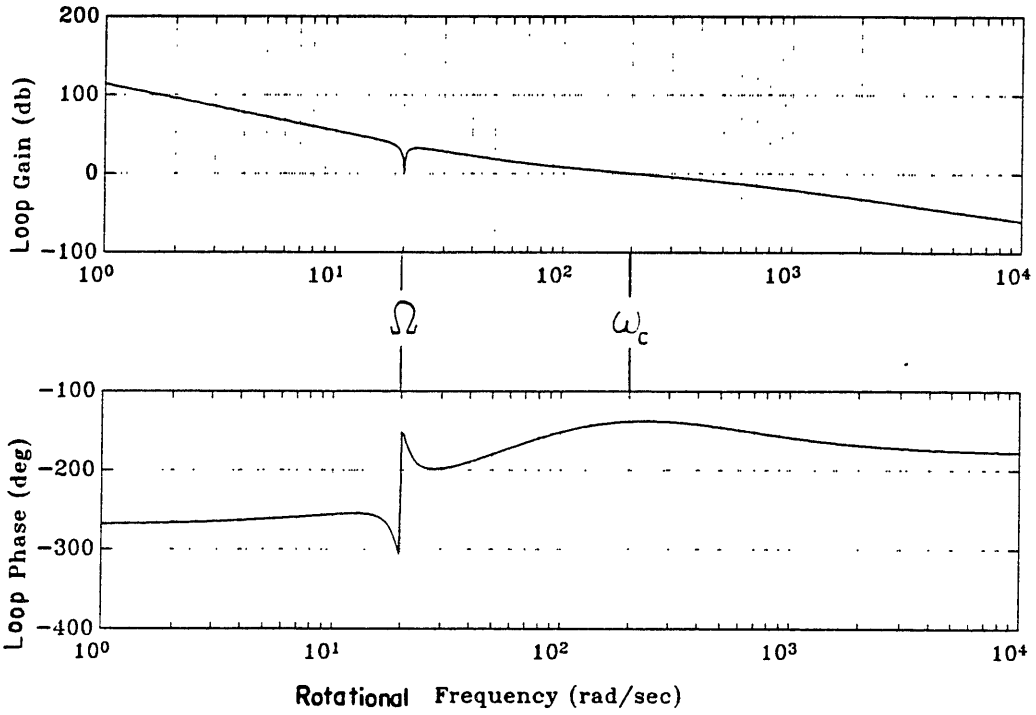

Figure 5.4. Loop Frequency Response, Rigid Rotor, Notch Filter Controller ($\Omega = .1\omega_c$)

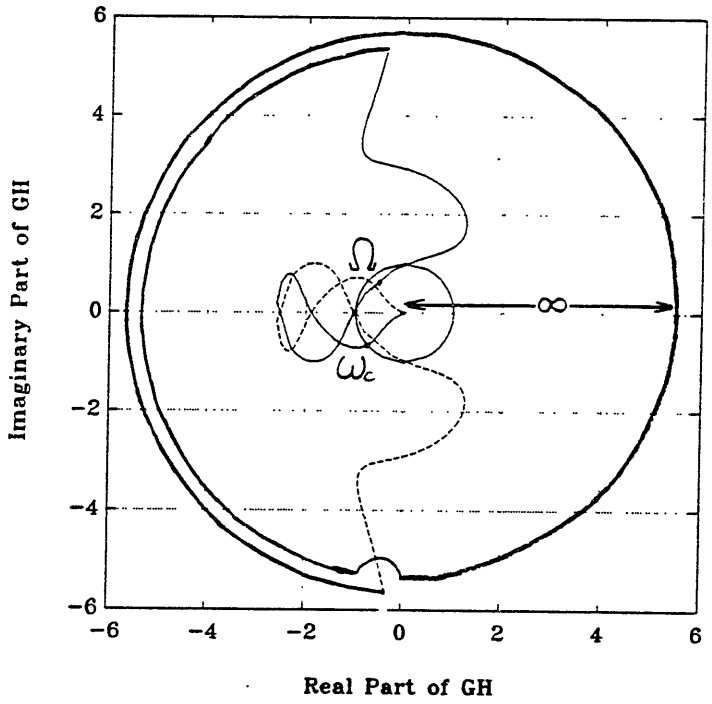

Figure 5.5. Loop Nyquist Plot, Rigid Rotor, Notch Filter Controller ($\Omega = .1\omega_c$)

frequencies of loop gain, causing encirclements of the point (-1 + 0j), resulting in an unstable system.

The range of frequencies between the point where the synchronous loop gain crosses over and the system goes unstable is a function of both the loop gain and phase of the conventional control loop and the notch filter design. Generally, the stable range of frequencies above the crossover frequency of the synchronous loop gain is small and depends on the loop phase of the conventional control loop being below -180 degrees at this point. When it is, the loop phase at both crossover frequencies of loop gain near Ω will also be below -180 degrees, not encircling the point (-1 + 0j).

The frequency at which synchronous loop gain crosses over is a function of the loop gain and notch depth. Selection of a notch filter which is not as deep as the one used above would decrease the unstable range of frequencies in two ways. First, the frequency at which the synchronous loop gain crosses over is increased as notch depth is decreased. Second, since deeper notch filters result in more phase shift at the frequencies neighboring the center frequency (reference Figure 4.1), the onset of instability with increasing rotational frequency would be delayed by using a less deep notch. However, by reducing the notch depth excessively, the performance is also reduced, as will be discussed later. By varying the notch Q factor, the distance between the two frequencies at which loop gain crosses over can be changed, but the phase at these frequencies remains unchanged (reference Figure 4.2), therefore having a negligible effect on the unstable speed range.

Figure 5.6 shows the loop gain and phase with the rotational frequency chosen as $\Omega = .2\omega_c$. The figure reveals that the first crossover of the loop gain corresponds to a loop phase of roughly -270 degrees. The second crossover, at a frequency slightly above Ω, has a

loop phase of more than -150 degrees. It is apparent from the Nyquist plot, shown in Figure 5.7, that the notch pulls the Nyquist curve to the inside of the point (-1 + 0j), adding two encirclements of that point and destabilizing the system.

The loop gain and phase of the system with a rotational frequency (Ω) identical to the crossover frequency (ω_c) is shown in Figure 5.8. The stability here is easier to determine because the loop gain crosses over at only one frequency. Since the loop gain at this frequency is slightly greater than -180 degrees, the system has positive phase margin and is stable. The Nyquist plot, given in Figure 5.9, shows that the curve now passes to the outside of the point (-1 + 0j), causing no encirclements and leaving the system stable. The rotational frequency at which the system becomes stable again may be decreased by increasing the phase margin of the conventional control loop. At higher values of rotational frequency, the effects of the notch filter are confined to the interior of the unit circle where it cannot affect system stability.

In summary, it has been shown that the range of unstable rotational frequencies begins just after the synchronous loop gain (loop gain at Ω) crosses over (reference Figure 5.2). This frequency may be increased by decreasing the notch depth. The unstable region ends just before the rotational frequency (Ω) equals the crossover frequency of the conventional control loop (ω_c).

By plotting loop phase and gain margins as functions of normalized rotational frequency (Ω/ω_c), the results of the Nyquist plots may be shown on a single figure, as given in Figure 5.10. From the Nyquist plots, the phase margin may be interpreted as the angle from -180 degrees that the curve crosses the unit circle. Positive phase margin corresponds to the curve entering the unit circle with more than -180 degrees phase, i.e. below the point (-1 + 0j). Likewise, the gain margin is the distance from the point

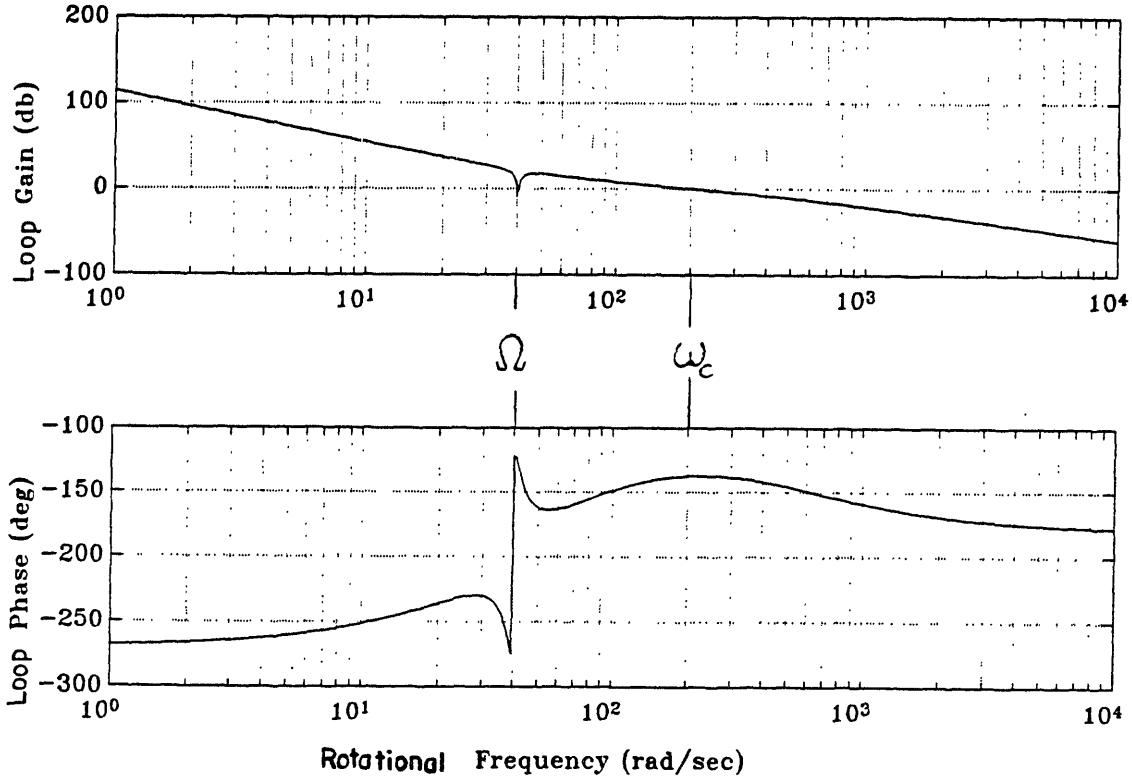

Figure 5.6. Loop Frequency Response, Rigid Rotor, Notch Filter Controller ($\Omega = .2\omega_c$)

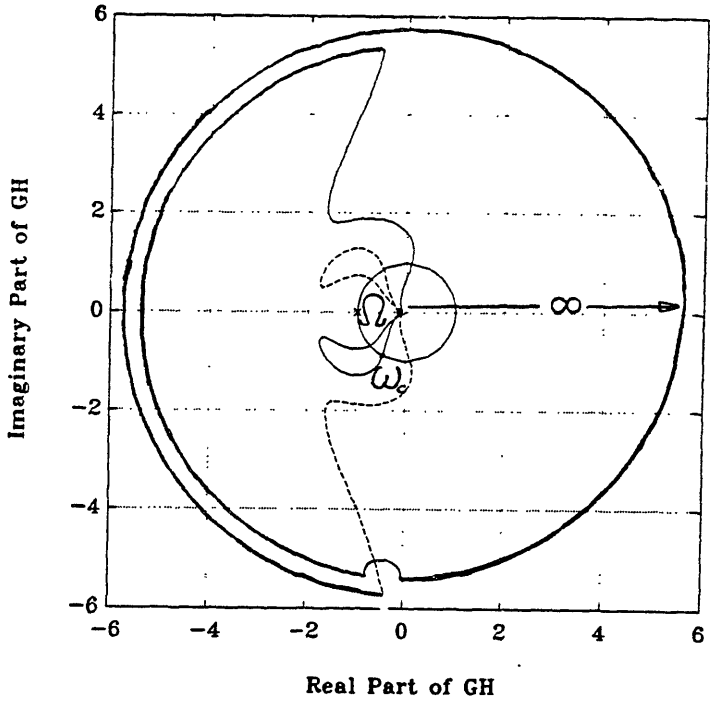

Figure 5.7. Loop Nyquist Plot, Rigid Rotor, Notch Filter Controller ($\Omega = .2\omega_c$)

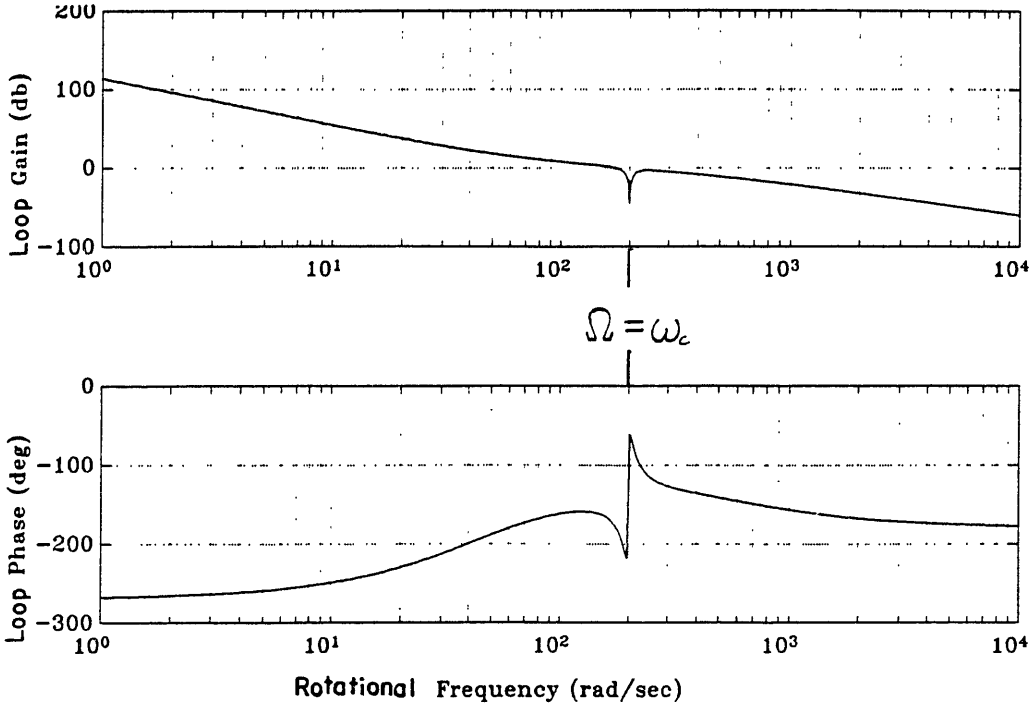

Figure 5.8. Loop Frequency Response, Rigid Rotor, Notch Filter Controller ($\Omega = \omega_c$)

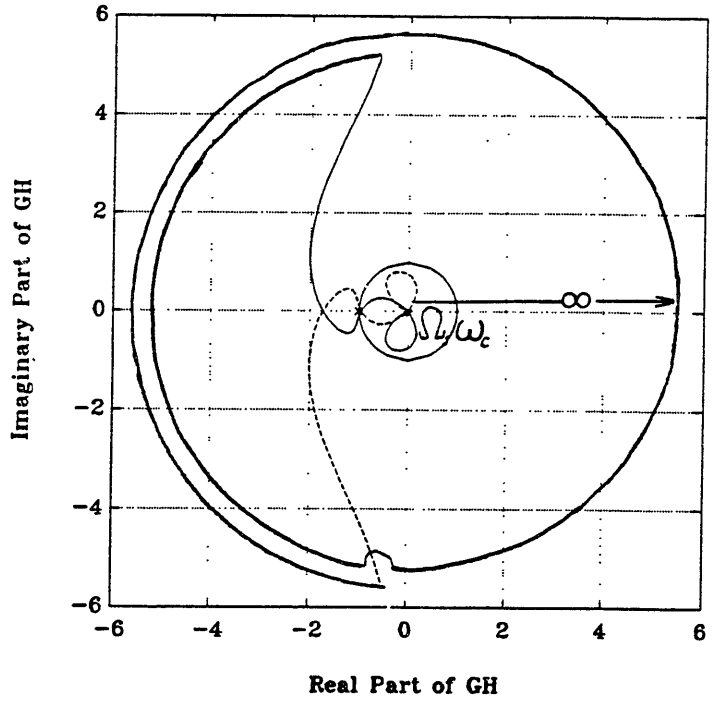

Figure 5.9. Loop Nyquist Plot, Rigid Rotor, Notch Filter Controller ($\Omega = \omega_c$)

(-1 + 0j) along the negative real axis to the intersection of the curve and the axis, where positive gain margin represents intersection of the curve and the real axis inside the unit circle. As shown in Figure 5.10, there can be multiple values of both phase and gain margin. Gain margin has a single value at low frequencies but has three after the part of the Nyquist curve representing the notch filter dips below the negative real axis, giving two additional intersections. The phase margin has a single constant value until the synchronous loop gain crosses over (the curve first dips inside the unit circle). At that point, two additional values of phase margin appear. The unstable region begins when one value each of the phase and gain margin changes sign, as indicated on the figure. This signifies the Nyquist curve crossing to the inside of the

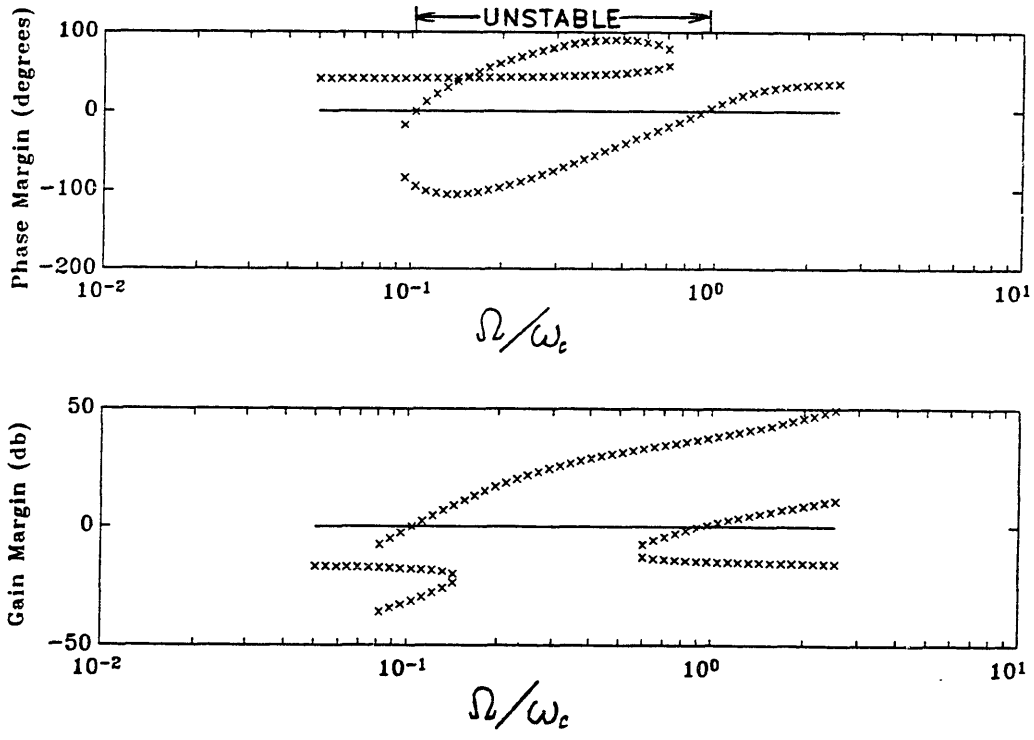

Figure 5.10. Phase and Gain Margins versus Normalized Rotational Frequency, Rigid Rotor, Notch Filter Controller

point (-1 + 0j) for the first time. The unstable region ends when all values of the phase margin become positive again, corresponding to no encirclements of the point (-1 + 0j). All values of the gain margin but one become positive for high rotational frequency, representing the effects of the notch filter entering the interior of the unit circle.

The stability can also be thought of in terms of eigenvalue damping and frequency as functions of rotational frequency, as shown in Figures 5.11 and 5.12. These plots are derived from the root locus as a function of rotational frequency. Figure 5.11 shows that the minimum eigenvalue damping approaches the numerator damping factor of the tracking notch filter (ξ_n) at low rotational frequency. For the nominal notch filter design, the numerator damping factor (ξ_n) equals 0.001 and the denominator damping factor (ξ_d) equals 0.1. As rotational frequency is increased and exceeds the crossover frequency of the synchronous loop gain, the minimum eigenvalue damping becomes negative, destabilizing the system. Above the crossover frequency (ω_c), the minimum eigenvalue damping becomes positive and approaches the value of the notch denominator damping factor (ξ_d), giving a stable system. Figure 5.12 shows that one eigenvalue frequency equals the rotational frequency whereas the other is roughly equal to the crossover frequency (ω_c). It is no surprise that these poles, generated by the notch filter, are responsible for determining the system stability.

These results may be shown algebraically by writing the characteristic equation and simplifying for extreme values of rotational frequency (Ω). Since the synchronous frequency is of interest, the value of the frequency (ω) is assumed identical to that of the rotational frequency (Ω). For small values of Ω, higher order terms of Ω and ω may be ignored, leaving as the characteristic equation:

$$s^2 + 2\Omega\xi_n s + \Omega^2 = 0 \qquad 5.1$$

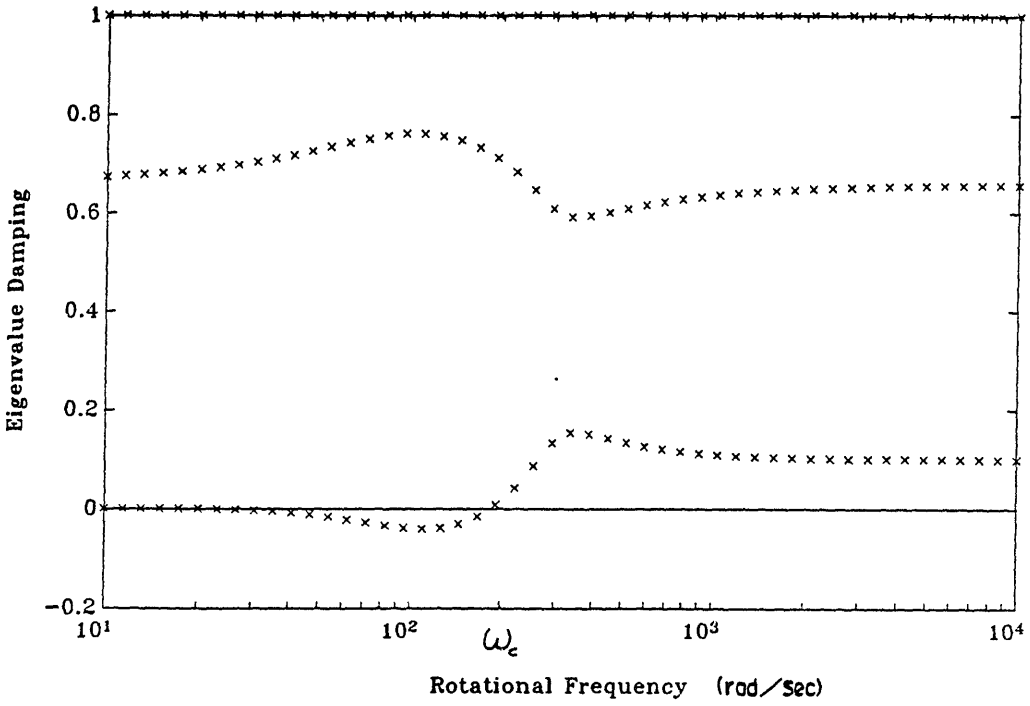

Figure 5.11.Eigenvalue Damping versus Rotational Frequency, Rigid Rotor, Notch Filter Controller

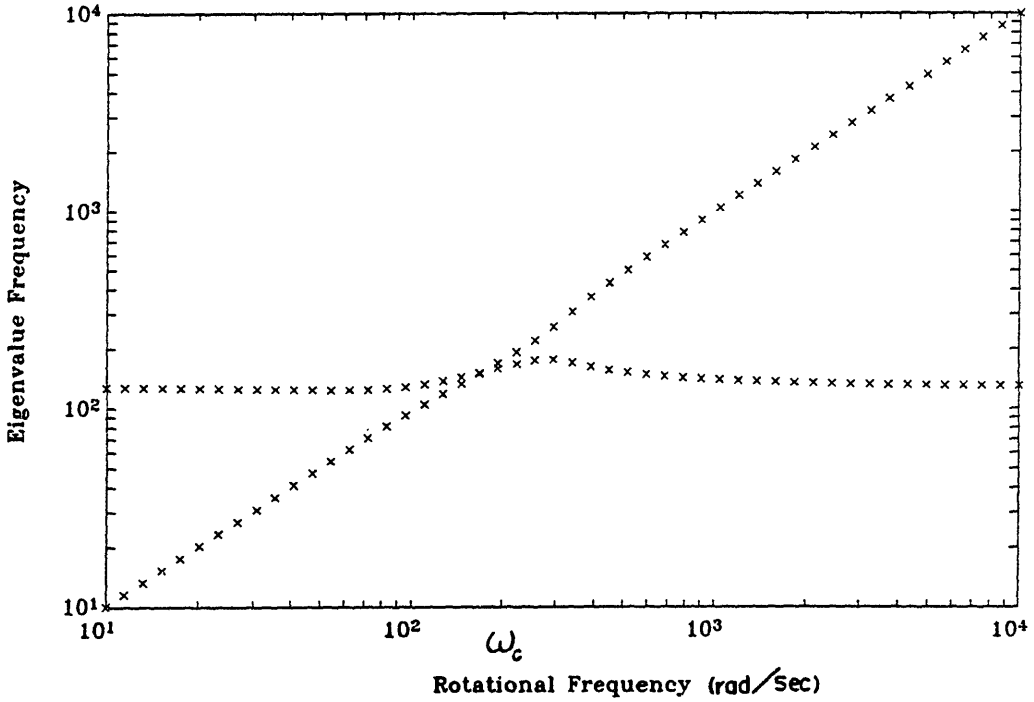

Figure 5.12. Eigenvalue Frequency versus Rotational Frequency, Rigid Rotor, Notch Filter Controller

where $s = j\omega$. For large values of rotational frequency, only the higher order terms of Ω and ω are kept and the rest are ignored, leaving:

$$s^2 + 2\Omega\xi_d s + \Omega^2 = 0. \qquad 5.2$$

The transient response of this system to a unit step input in bearing position reference for a rotational frequency of $\Omega = 2\omega_c$ is given in Figure 5.13. This value of rotational frequency is chosen because the notch filter has little effect on the overall stability once it is substantially above the crossover frequency (ω_c). The step response for rotational frequencies below the crossover of synchronous loop gain, i.e. the low speed stable region, is similar since the notch filter does not affect stability in this range of frequencies either. The phase margin is constant for values of rotational frequency above ω_c, as seen in Figure 5.10.

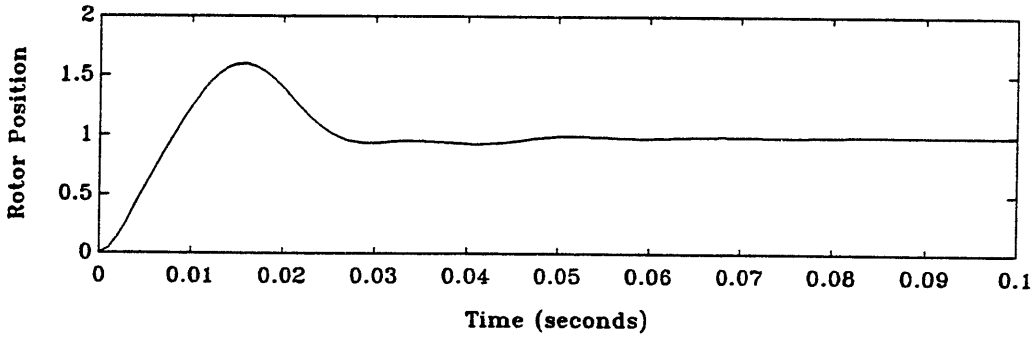

Figure 5.13. Unit Step Response, Rigid Rotor, Notch Filter Controller ($\Omega = 2\omega_c$)

5.2. Flexible Rotor Control System

5.2.1. Bearing Position Feedback

Notch filter control of a rotor system for which the shaft is relatively stiff compared to the bearings has essentially the same stability characteristics as for the previous system, in which shaft flexibility is ignored. As shown in Chapter 3, the effect of the resonance induced by shaft flexure is entirely within the unit circle and has no effect on system stability (reference Figure 3.6).

The following pages will focus on the stability of the system with a soft shaft relative to the bearings and the addition of the tracking notch filter. Bearing feedback will be examined here and rotor feedback in the next section. The approach here will be identical to the one used above. Using the nominal notch filter, rotational frequency will be increased while periodically observing the loop gain and phase and Nyquist plot for changes in stability.

At low values of rotational frequency (Ω), the system is stable. Figure 5.14 shows the loop gain and phase with the rotational frequency (Ω) chosen relative to the flexible frequency (ω_s) to be $\Omega = .05\omega_s$. As before, the system is stable for frequencies below the crossover of the synchronous loop gain. The Nyquist plot is shown in Figure 5.15. As previously mentioned in Chapter 3, low frequency integral control action was omitted from this controller, causing the Nyquist curve to approach the origin at low frequency along the negative real axis, corresponding to a phase of -180 degrees (reference Figure 3.8). The effect of the notch filter is, once again, to pull the Nyquist curve toward the origin at Ω, giving a clockwise phase shift at frequencies below Ω and a counterclockwise phase shift above Ω. At low values of rotational frequency, the curve enters the unit circle at approximately the same location as when the notch filter was omitted from the

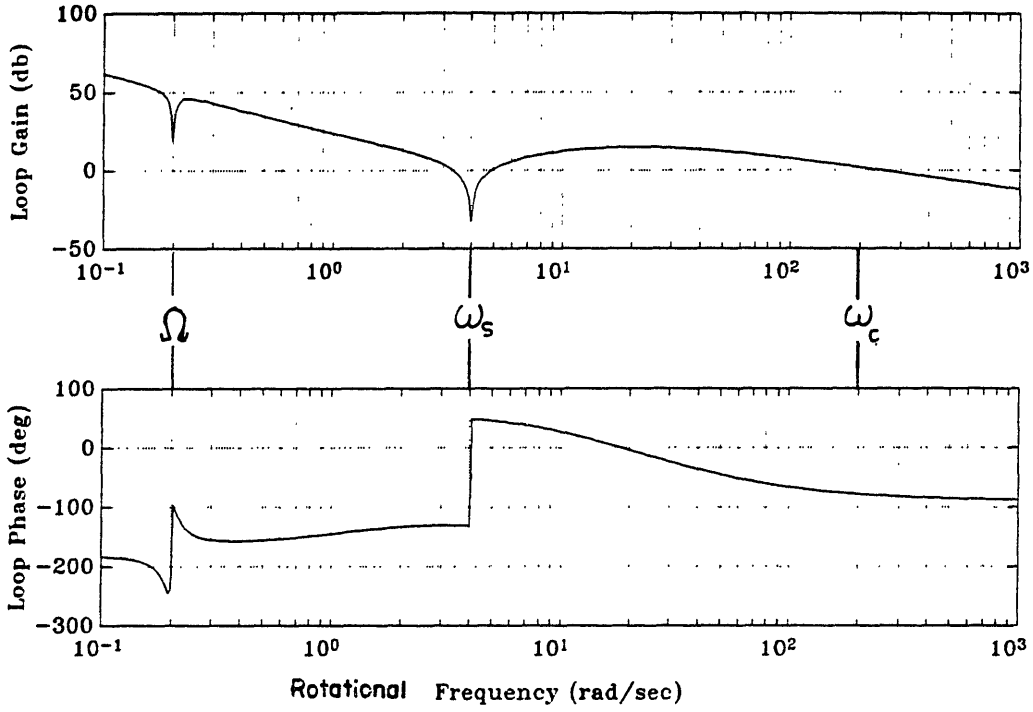

Figure 5.14. Loop Frequency Response, Flexible Rotor (Soft Shaft), Bearing Feedback ($\Omega = .05\omega_s$)

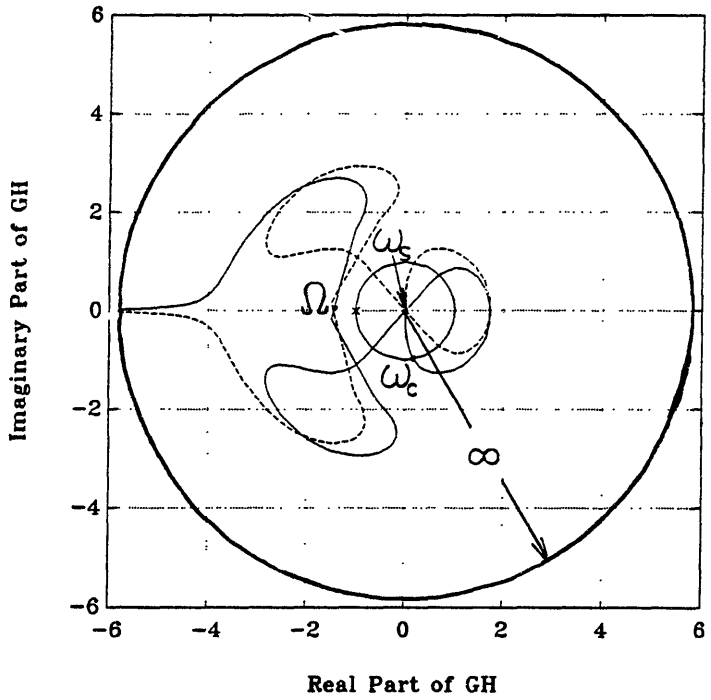

Figure 5.15. Loop Nyquist Plot, Flexible Rotor (Soft Shaft), Bearing Feedback ($\Omega = .05\omega_s$)

controller, resulting in no encirclements and a stable system.

Figure 5.16 shows the loop gain and phase for $\Omega = .1\omega_s$. At this value of rotational frequency, the synchronous loop gain is below unity. The two crossover frequencies of loop gain near Ω correspond to values of loop phase which straddle -180 degrees. The Nyquist plot, given in Figure 5.17, shows that the point (-1 + 0j) becomes encircled almost immediately after the synchronous loop gain crosses over. This is because the loop phase of the conventional controller is -180 degrees at low frequency. The lack of low frequency integral action also causes the crossover frequency of the synchronous loop gain to be reduced by reducing the loop gain of the conventional controller. Therefore, the unstable region of rotational frequencies is slightly larger than for the rigid rotor system examined above.

Figure 5.18 shows the loop gain and phase for the rotational frequency equal to the flexible frequency. The crossover frequencies of loop gain correspond to values of loop phase above -180 degrees. The Nyquist plot, in Figure 5.19, shows that the curve once again passes beneath the point (-1 + 0j), giving a stable system. The system remains stable for rotational frequencies above the flexible frequency (ω_s) because loop phase of the conventional controller remains above -90 degrees. This is shown in Figure 5.20, for which $\Omega = 5\omega_s$. Since the maximum phase excursion due to the notch filter is 90 degrees, the loop phase at the crossover frequencies of loop gain never drop below -180 degrees. In terms of the Nyquist plot, shown in Figure 5.21, the effect of the notch filter will be restricted to the positive real half and negative imaginary half of the s-plane, not allowing any encirclements of the point (-1 + 0j).

Figure 5.22 gives the minimum eigenvalue damping of the soft shaft system with bearing feedback as a function of

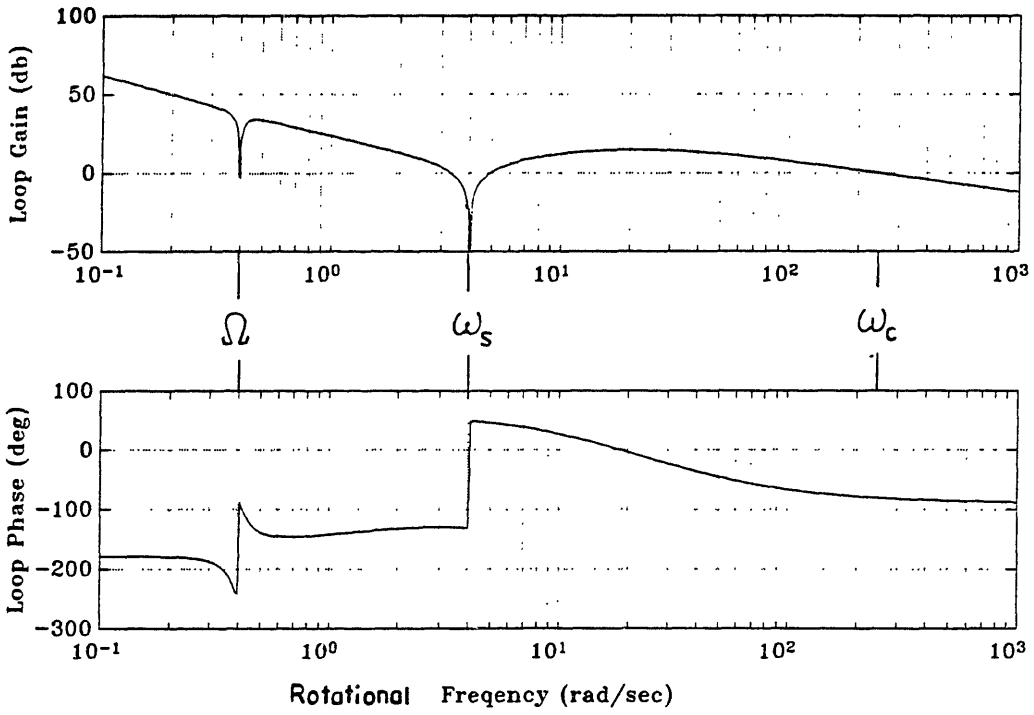

Figure 5.16. Loop Frequency Response, Flexible Rotor (Soft Shaft), Bearing Feedback ($\Omega = .1\omega_s$)

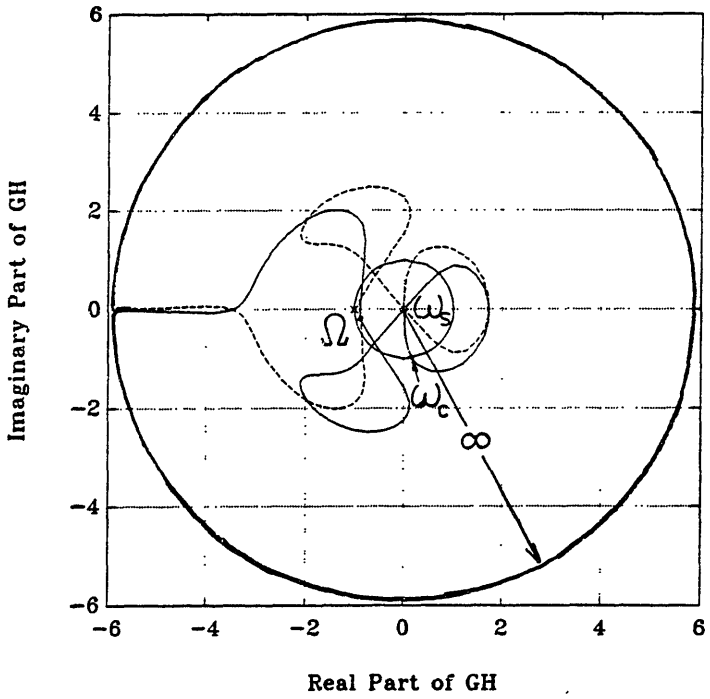

Figure 5.17. Loop Nyquist Plot, Flexible Rotor (Soft Shaft), Bearing Feedback ($\Omega = .1\omega_s$)

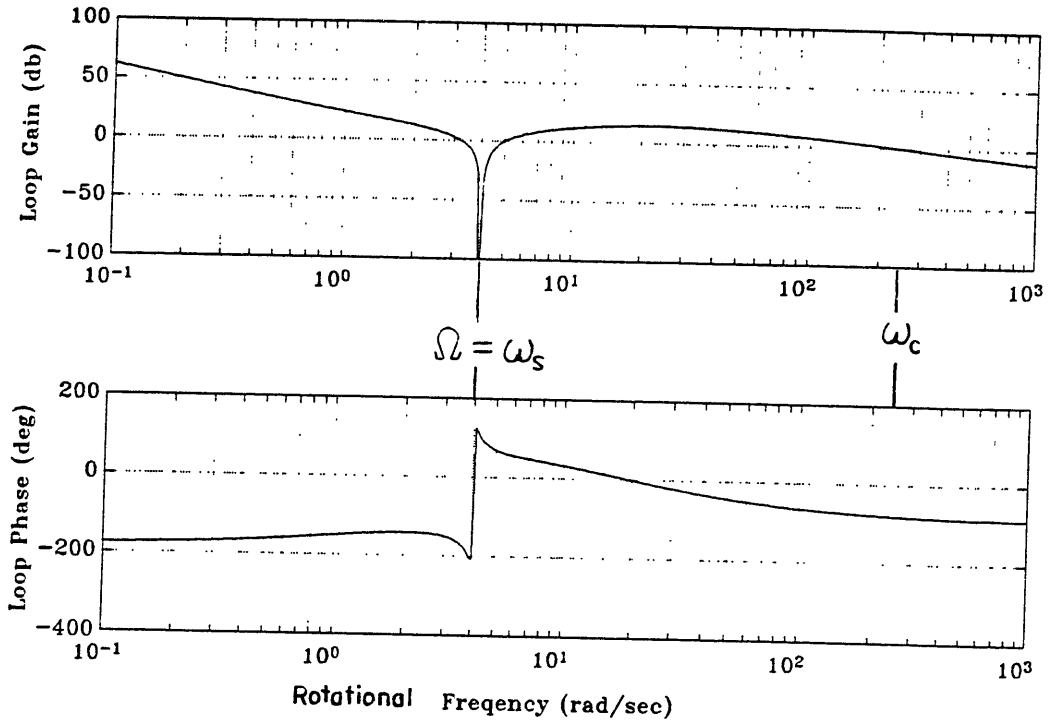

Figure 5.18. Loop Frequency Response, Flexible Rotor (Soft Shaft), Bearing Feedback ($\Omega = \omega_s$)

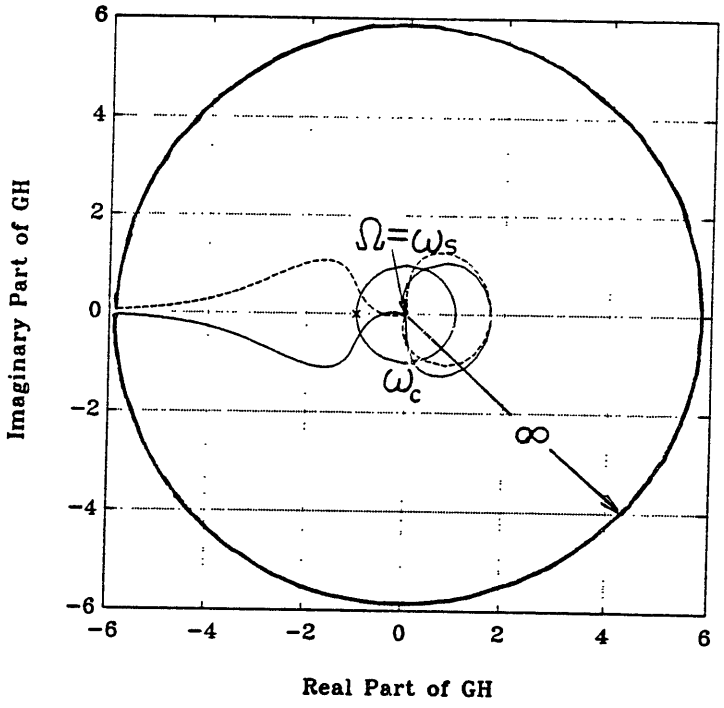

Figure 5.19. Loop Nyquist Plot, Flexible Rotor (Soft Shaft), Bearing Feedback ($\Omega = \omega_s$)

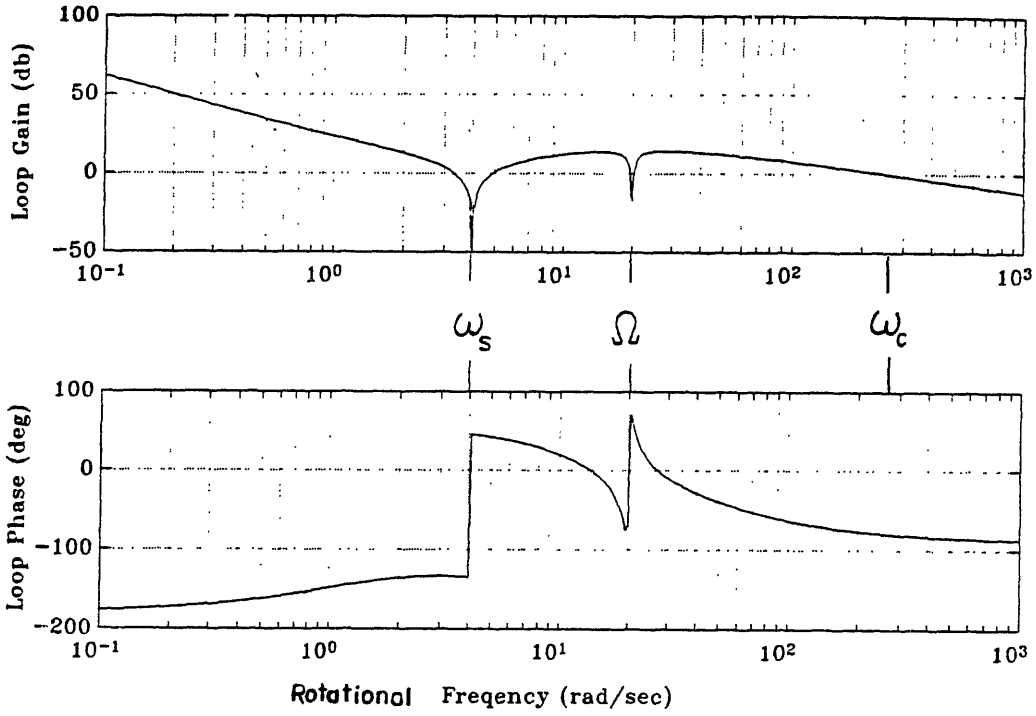

Figure 5.20. Loop Frequency Response, Flexible Rotor (Soft Shaft), Bearing Feedback ($\Omega = 5\omega_s$)

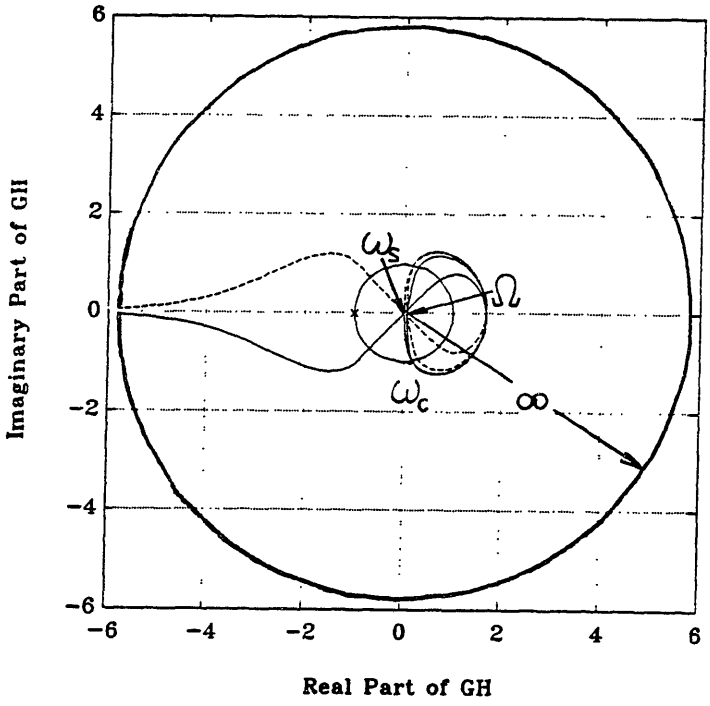

Figure 5.21. Loop Nyquist Plot, Flexible Rotor (Soft Shaft), Bearing Feedback ($\Omega = 5\omega_s$)

normalized rotational frequency (Ω/ω_s). It shows that the minimum eigenvalue damping equals the notch numerator damping factor (ξ_n) at low frequency and becomes negative between the crossover of the synchronous loop gain and the flexible frequency (ω_s), similarly to the rigid rotor system. At super-flexible frequencies however, instead of approaching the value of the notch denominator damping factor (ξ_d), the minimum eigenvalue damping is much lower. This is because the low phase margin at the flexible frequency provides an eigenvalue with damping lower than that of the notch filter open loop pole.

The low phase margin at the flexible frequency (ω_s) can be seen in the response of the rotor position to a unit step in bearing position reference for a rotational frequency of $\Omega = 5\omega_s$, given in Figure 5.23. The rotor position rings at approximately 3.2 radian/second, the value of the crossover frequency just below the flexible frequency (ω_s) (reference Figure 5.20). The low phase margin at this frequency causes the system to undergo lightly damped oscillations at this frequency. Loop phase may be increased at this frequency by increasing the extent of derivative control action, however, this would increase the frequency at which the bearing position rolls off (the highest crossover frequency shown in Figure 5.20). This should be avoided since it has an adverse effect on the system performance, as will be discussed in the chapter on system performance.

5.2.2. Rotor Position Feedback

Ignoring the effects of spillover in this simple model, the same rotor system as used above can be stabilized more effectively by using the rotor position instead of bearing position for feedback. Although the shaft is soft compared to the bearings, the loop transfer function has no resonance at the flexible frequency (ω_s) because the effects of the shaft flexibility are not seen by the

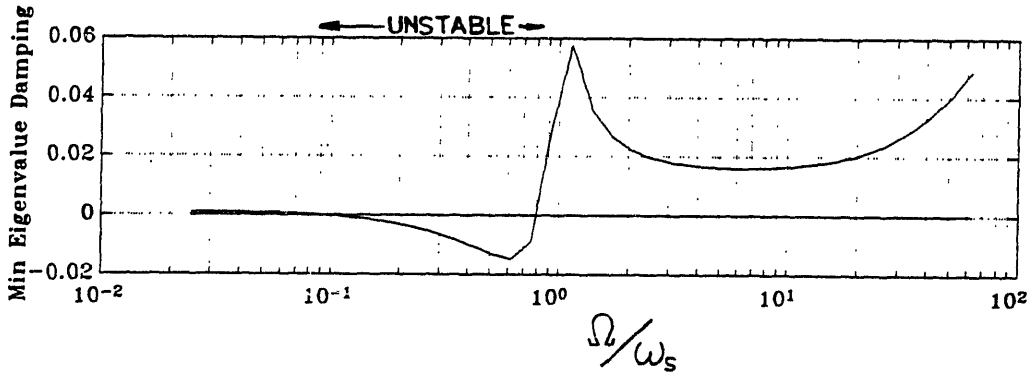

Figure 5.22. Minimum Eigenvalue Damping versus Normalized Rotational Frequency, Flexible Rotor (Soft Shaft), Bearing Feedback

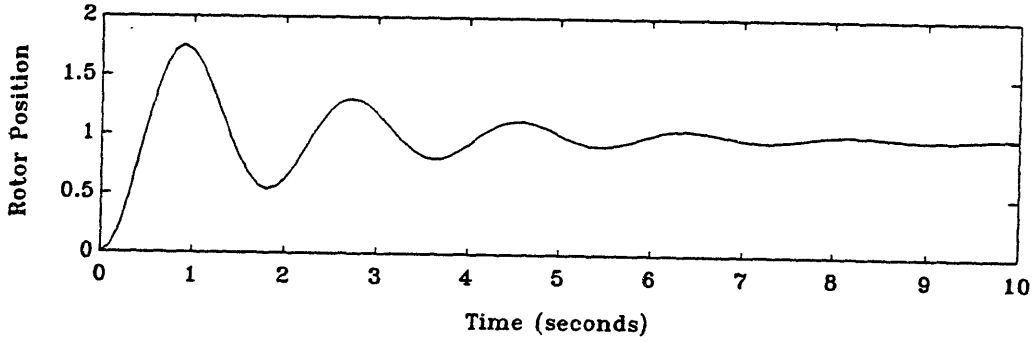

Figure 5.23. Unit Step Response, Flexible Rotor (Soft Shaft), Bearing Feedback ($\Omega = 5\omega_s$)

controller (reference Figure 3.9).

The effect of the nominal notch filter design on system stability is basically the same as for the rigid rotor system studied previously. Figure 5.24 shows the loop gain and phase with a rotational frequency of $\Omega = .05\omega_c$. The Nyquist plot, in Figure 5.25, shows that the synchronous loop gain has not crossed over, resulting in no encirclements of the point (-1 + 0j).

Figure 5.26, showing loop gain and phase for rotational frequency of $\Omega = .1\omega_c$, reveals that synchronous loop gain has crossed over at this rotational frequency. As for the soft shaft controller with bearing feedback, the unstable region begins immediately after synchronous loop gain has crossed over, as seen in Figure 5.27.

Figure 5.28, loop gain and phase for rotational frequency of $\Omega = \omega_c$, shows only one crossover frequency of loop gain with a corresponding loop phase of more than -180 degrees. Figure 5.29, the Nyquist plot, shows that the system has become stable again and the effect of the notch filter has entered the interior of the unit circle.

Figure 5.30 shows that the minimum eigenvalue damping as a function of normalized rotational frequency (Ω/ω_c) is similar to that of the rigid rotor system, shown in Figure 5.11. The minimum eigenvalue damping above the loop crossover frequency (ω_c) approaches the value of the notch filter denominator damping factor (ξ_d). For rotor feedback, there is sufficient phase margin at the flexible frequency (ω_c) since the resonance at this frequency is not seen by the controller.

Figure 5.31 shows the response of rotor position in this system to a unit step in rotor position reference for a rotational frequency of $\Omega = 2\omega_c$ (the same frequency as for the step response of the bearing feedback system, shown in Figure 5.23). The ringing at the flexible frequency is much reduced, another indication that the phase margin at this frequency is better than for the system with bearing

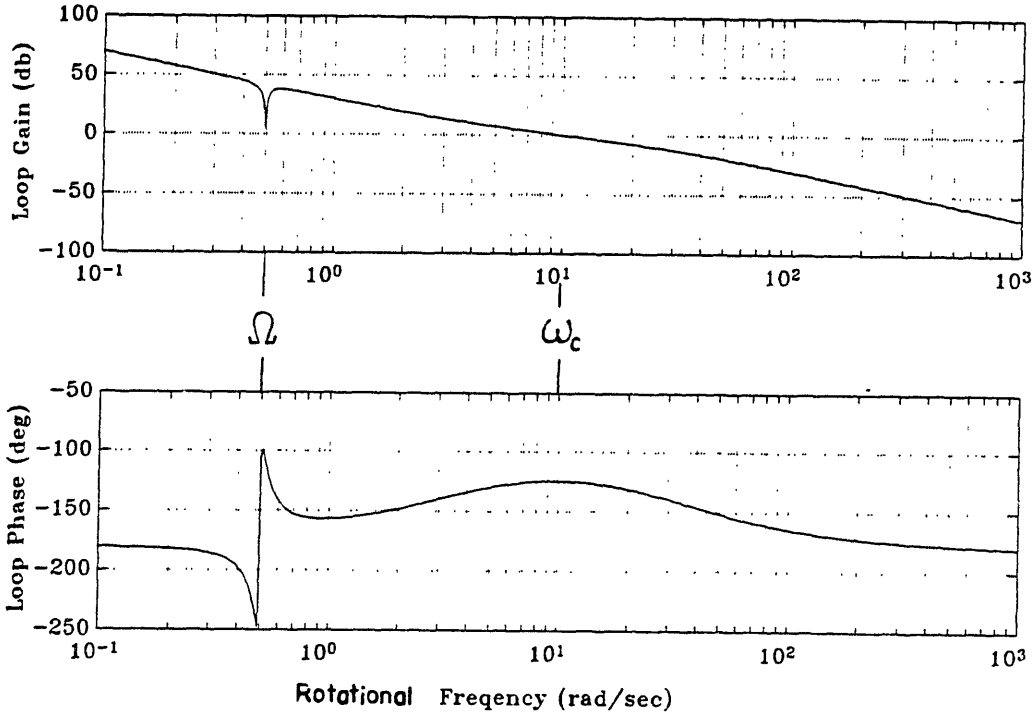

Figure 5.24. Loop Frequency Response, Flexible Rotor (Soft Shaft), Rotor Feedback ($\Omega = .05\omega_c$)

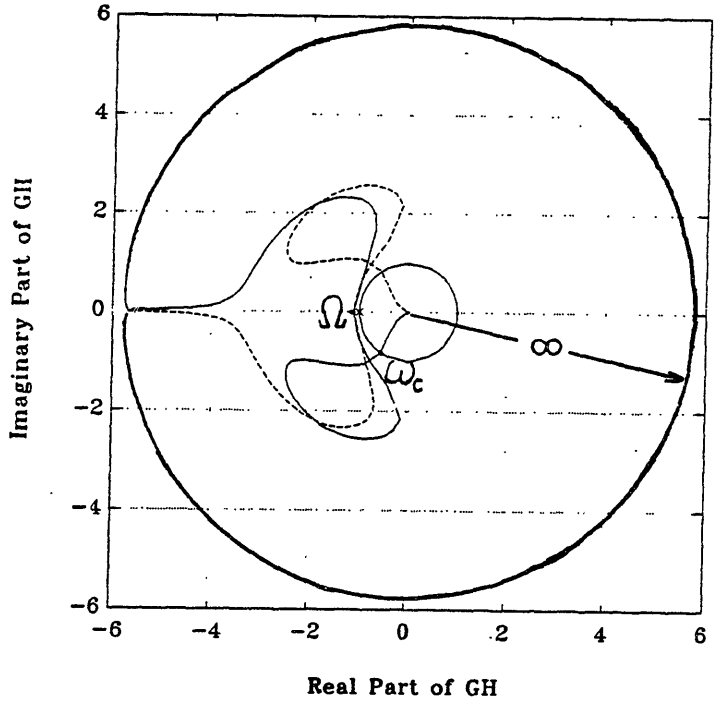

Figure 5.25. Loop Nyquist Plot, Flexible Rotor (Soft Shaft), Rotor Feedback ($\Omega = .05\omega_c$)

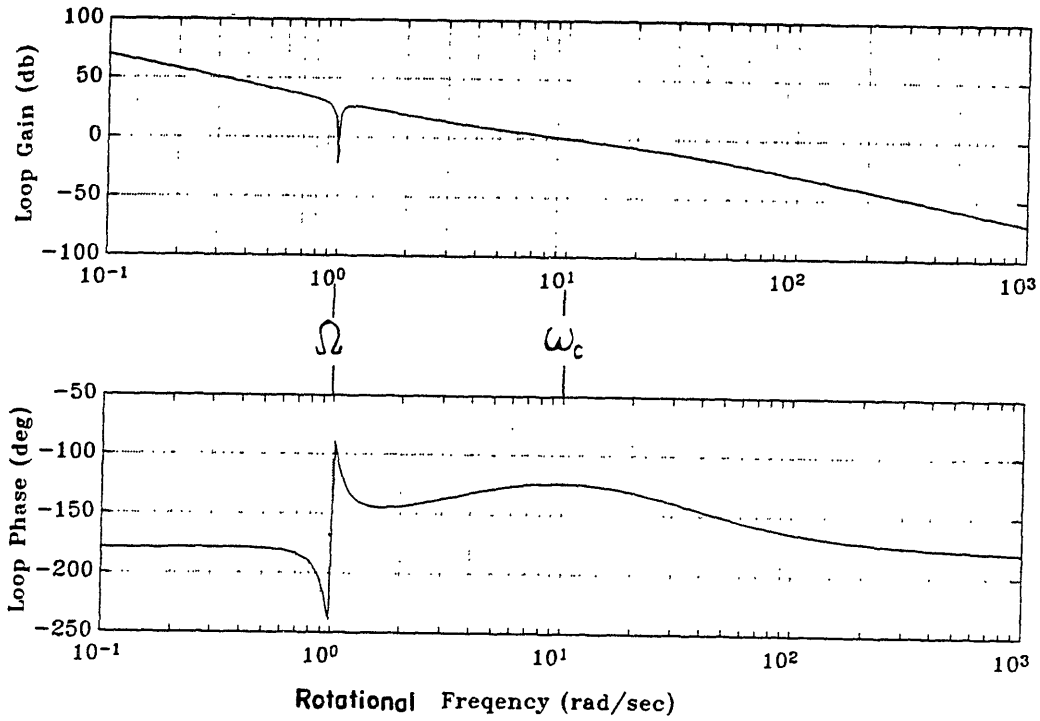

Figure 5.26. Loop Frequency Response, Flexible Rotor (Soft Shaft), Rotor Feedback ($\Omega = .1\omega_c$)

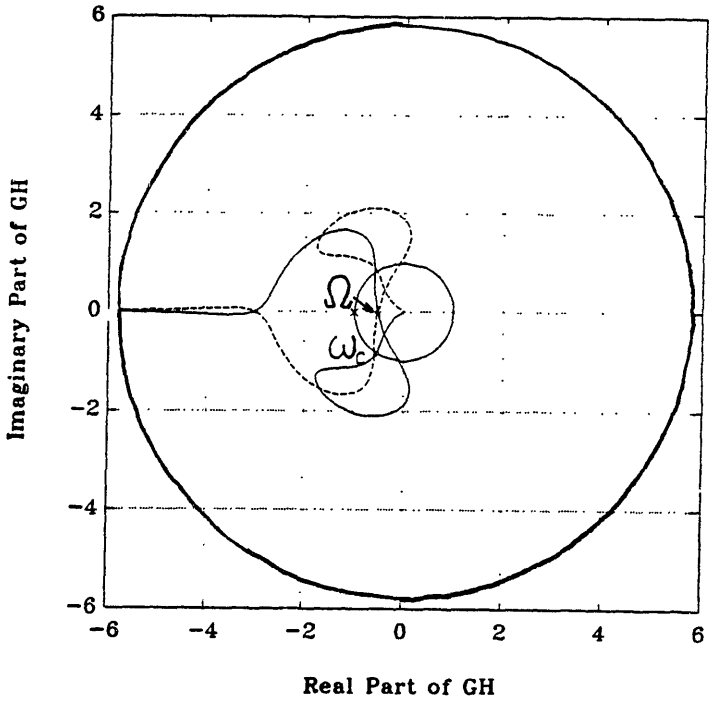

Figure 5.27. Loop Nyquist Plot, Flexible Rotor (Soft Shaft), Rotor Feedback ($\Omega = .1\omega_c$)

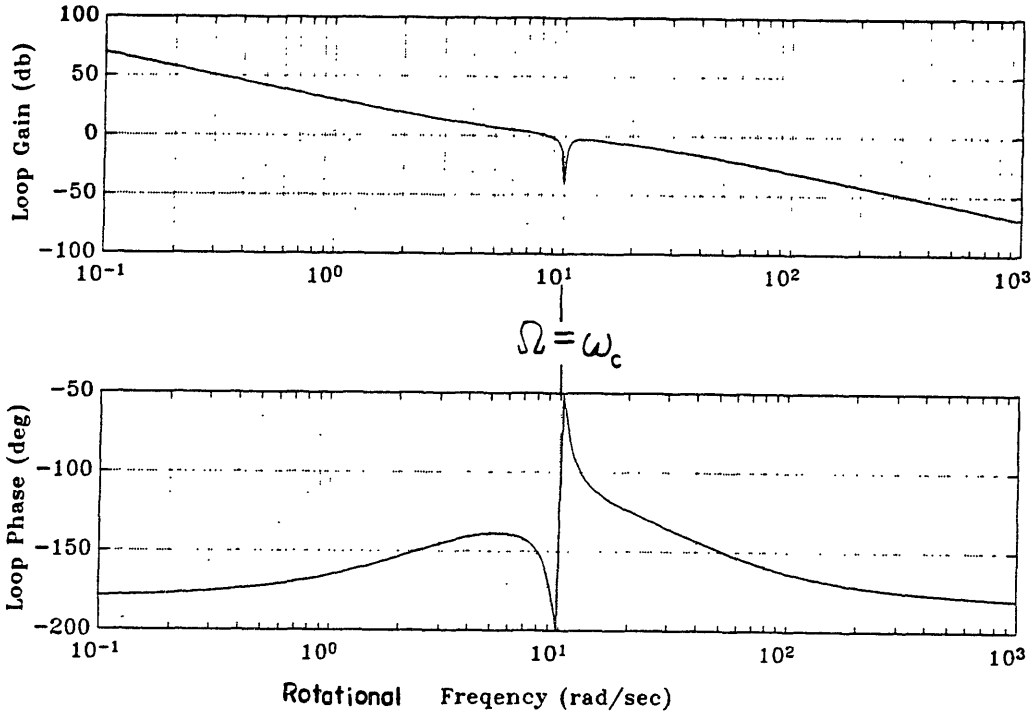

Figure 5.28. Loop Frequency Response, Flexible Rotor (Soft Shaft), Rotor feedback ($\Omega = \omega_c$)

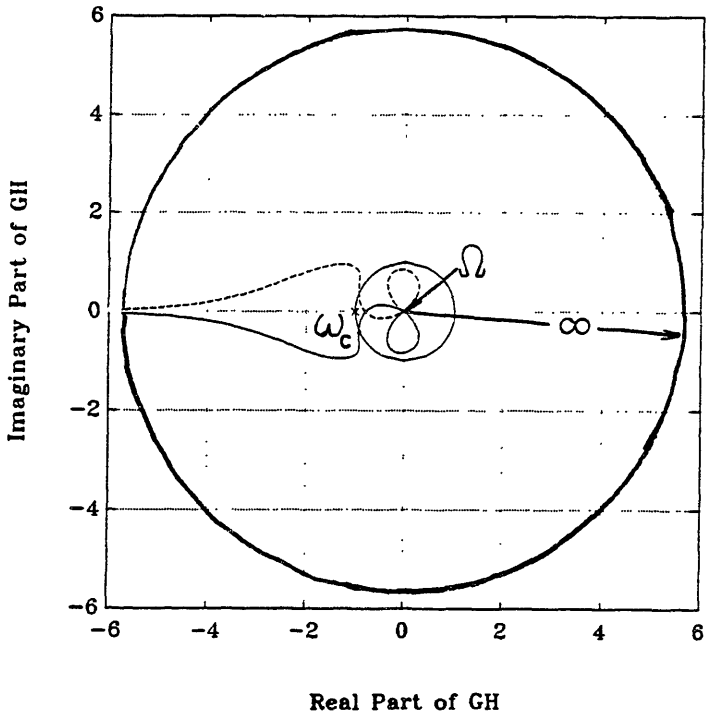

Figure 5.29. Loop Nyquist Plot, Flexible Rotor (Soft Shaft), Rotor Feedback ($\Omega = \omega_c$)

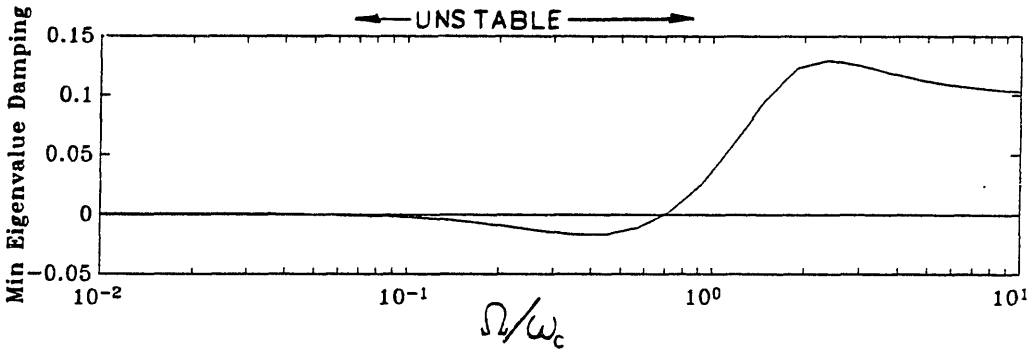

Figure 5.30. Minimum Eigenvalue Damping versus Normalized Rotational Frequency, Flexible Rotor (Soft Shaft), Rotor Feedback

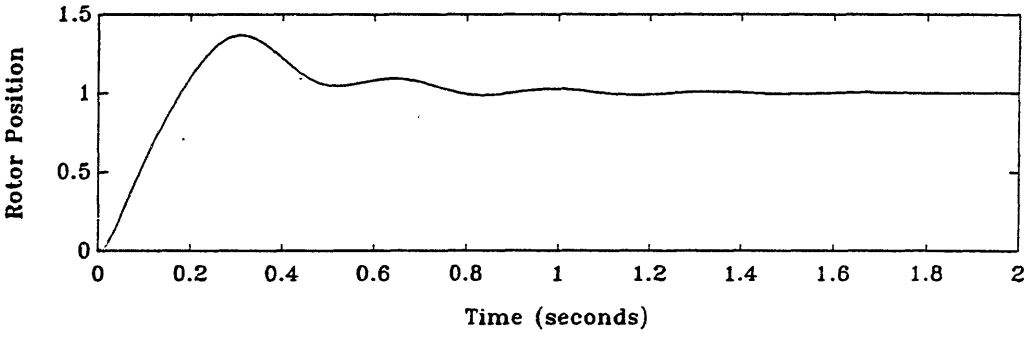

Figure 5.31. Unit Step Response, Flexible Rotor (Soft Shaft), Rotor Feedback ($\Omega = 2\omega_c$)

feedback.

In summary, the range of rotational frequencies of the flexible rotor system for which the notch filter destabilizes the system lies just below the lowest critical frequency of the loop. The lowest critical frequency is the flexible frequency (ω_s) for systems with bearing feedback and soft shaft relative to the bearings, since the flexible frequency occurs below the crossover frequency (ω_c). Conversely, the lowest critical frequency is the crossover frequency when the shaft is stiff relative to the bearings. Systems with rotor feedback are unstable for values of rotational frequency just below the crossover frequency, regardless of shaft stiffness since the shaft flexible frequency is not a critical frequency in the loop transfer function. Generally, the range of unstable frequencies extends from the lowest crossover frequency of synchronous loop gain to the lowest critical frequency, either the loop crossover frequency (ω_c) or the shaft flexible frequency (ω_s).

CHAPTER 6
NOTCH FILTER CONTROLLER PERFORMANCE

The purpose of the notch filter controller is to allow the center of mass to remain stationary by making the bearings not respond at the rotational frequency. This chapter will examine the effectiveness of the notch filter in reducing the response of the rotor center of mass to the synchronous forcing function caused by mass imbalance. One measure of performance of the notch filter controller is the synchronous closed loop transfer function from synchronous forcing function to center of mass position. The difference in attenuation of the synchronous disturbance by the notch filter controller and by the conventional controller will be used in this chapter to define the performance of the notch filter controller.

6.1. Rigid Rotor System

Figure 6.1 shows the synchronous closed loop gain of the rigid rotor system with the two types of controller (conventional and notch filter), measured from synchronous forcing function to center of mass position. The closed loop transfer function of a single input, single output feedback system is defined as:

$$G_{cl} = \frac{G}{1 + GH} \qquad 6.1$$

where G represents the feedforward transfer function and H represents the feedback transfer function. The feedback transfer function of this particular system is unity (reference Figure 2.3) and the feedforward transfer function is equivalent to the synchronous loop gain. The derivation of the synchronous closed loop transfer function is addressed further in Appendix B. Recall that the synchronous loop gain is identical to loop gain when the

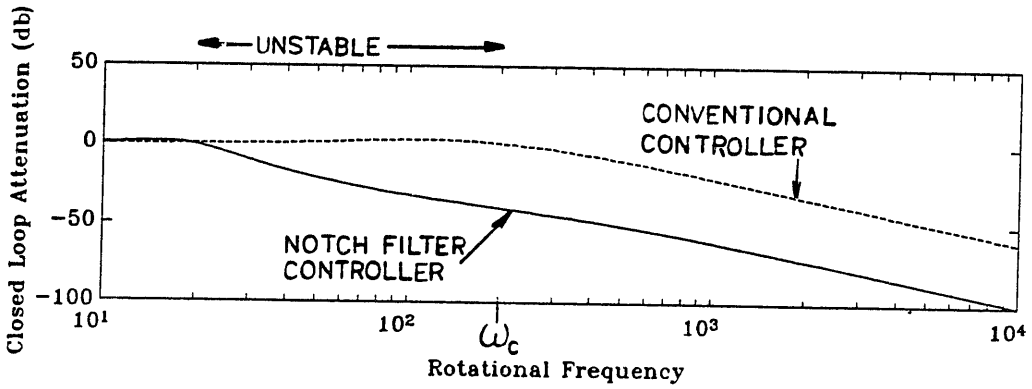

Figure 6.1. Synchronous Closed Loop Gain, Rigid Rotor, Conventional and Notch Filter Controllers

controller has no tracking notch filter, i.e. no dependence on rotational frequency. For rotational frequencies well below the crossover frequency of loop gain (ω_c), the synchronous loop gain is large (reference Figure 3.1). From equation 6.1, the synchronous closed loop gain (G_{cl}) is approximately unity at low frequency. For rotational frequencies substantially above the crossover frequency (ω_c), the synchronous loop gain is small, resulting in a synchronous closed loop gain approximately equal to the synchronous loop gain at high rotational frequencies.

The same rules apply in defining the synchronous closed loop gain of the rigid rotor model with a notch filter controller. The addition of the nominal notch filter with a depth of 40db places the synchronous loop gain uniformly 40db below the synchronous loop gain of the system with the conventional controller. As before, the synchronous closed loop gain is unity below the crossover of synchronous loop gain and equal to the synchronous loop gain above this frequency. From Figure 6.1, the synchronous closed loop gain of the system with notch filter controller is lower than the system with the conventional controller by the notch depth (40db) at high frequency and begins to

attenuate at the crossover frequency of synchronous loop gain rather than the crossover of loop gain (ω_c).

As was shown in Chapter 5, this system with a notch filter controller may not be operated for rotational frequencies extending approximately from the crossover of synchronous loop gain to the crossover of loop gain (ω) because of stability constraints. Since the notch filter controller is stable and effective in improving the system synchronous response only for rotational frequencies above the loop gain crossover frequency (ω_c), this defines the useful range of this controller. The amount of improvement in system synchronous response due to the notch filter is approximately equal to the notch depth in this useful range of rotational frequencies.

6.2. Flexible Rotor System

6.2.1. Bearing Position Feedback

The performance of a flexible rotor system in which the shaft is relatively stiff compared to the bearings is essentially identical to that of the rigid rotor system. The useful range of rotational frequencies of the notch filter controller includes rotational frequencies above the loop gain crossover frequency (ω_c).

The more interesting case is the flexible rotor system for which the shaft is soft relative to the bearings. The synchronous closed loop gain of this system with the conventional and notch filter controller is shown in Figure 6.2. The synchronous disturbance caused by mass imbalance begins to become attenuated by the conventional controller, as measured at the center of mass, for rotational frequencies above the flexible frequency (ω_s). The synchronous closed loop gain with the nominal notch filter controller begins to attenuate at the crossover frequency of synchronous loop gain but the improvement in performance is not fully equal to the notch depth until the rotational

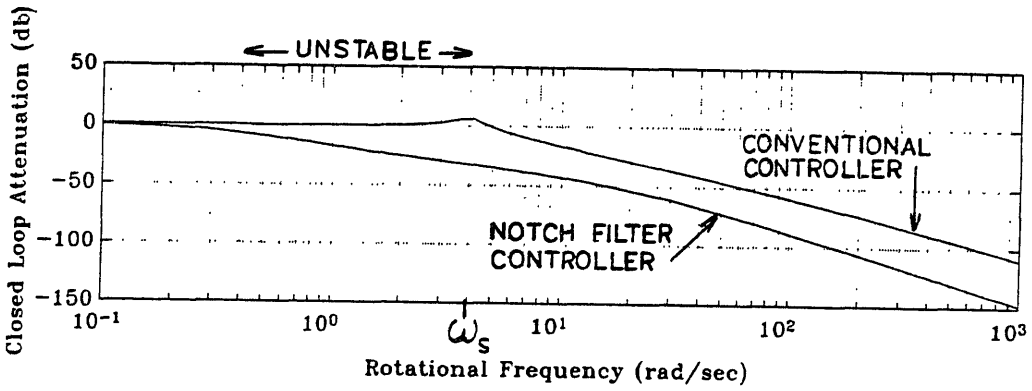

Figure 6.2. Synchronous Closed Loop Gain, Flexible Rotor (Soft Shaft), Conventional and Notch Filter Controllers

frequency (Ω) is much higher than the flexible frequency (ω_s).

Figure 6.3 shows a block diagram of this system where the following transfer functions are represented symbolically; the notch filter (G_n), the controller (G_c), the rotor (G_m) from bearing force (F_b) to center of mass position (Z_m) and the rotor (G_b) from bearing force to bearing center (Z_b). The synchronous closed loop transfer function of this system from synchronous forcing function caused by mass imbalance (D_s) to center of mass position (Z_m) is given as:

$$G_{cl} = \frac{Z_m}{D_s} = \frac{G_n G_c G_m}{1 + G_n G_c G_b} \qquad 6.2$$

The loop gain from synchronous forcing function to bearing position, $G_n G_c G_b$, for this system with a conventional controller, i.e. G_n equal to 1, is given in Figure 3.7. The loop gain from synchronous forcing function to center of mass position, $G_n G_c G_m$, with a conventional controller is shown in Figure 6.4. From these frequency responses, the magnitude of the synchronous closed loop gain, given in

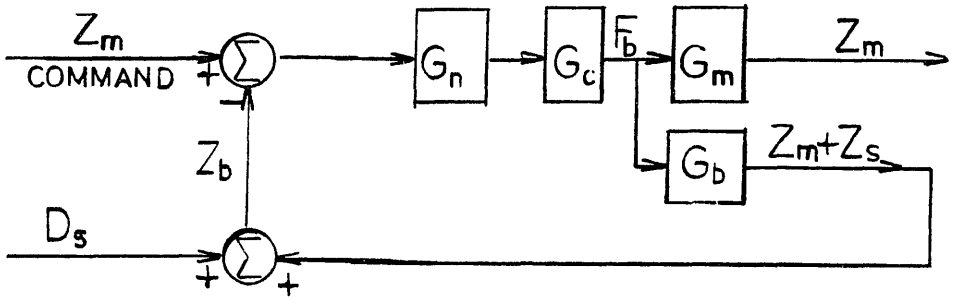

Figure 6.3. Block Diagram, Flexible Rotor System, Bearing Feedback, Notch Filter Control

equation 6.2, can be evaluated as a function of rotational frequency. The real quantity of interest is the amount of improvement the nominal notch filter provides as a function of rotational frequency. This is given by the ratio of the synchronous closed loop gain with the nominal notch filter to the synchronous closed loop gain without the notch filter, i.e. $G_n = 1$. The resulting expression is:

$$P_n = \frac{G_n(1 + G_cG_b)}{(1 + G_nG_cG_b)} \qquad 6.3$$

By evaluating the expression P_n as a function of rotational frequency, the improvement in performance due to the notch filter can be quantified. For rotational frequency well below the flexible frequency (ω_s), the term $G_nG_cG_b$ is large and the value of P_n is unity. Thus, at rotational frequencies well below the flexible frequency, the synchronous disturbance is not attenuated with a conventional controller or with a notch filter controller (reference Figure 6.2). At very high rotational

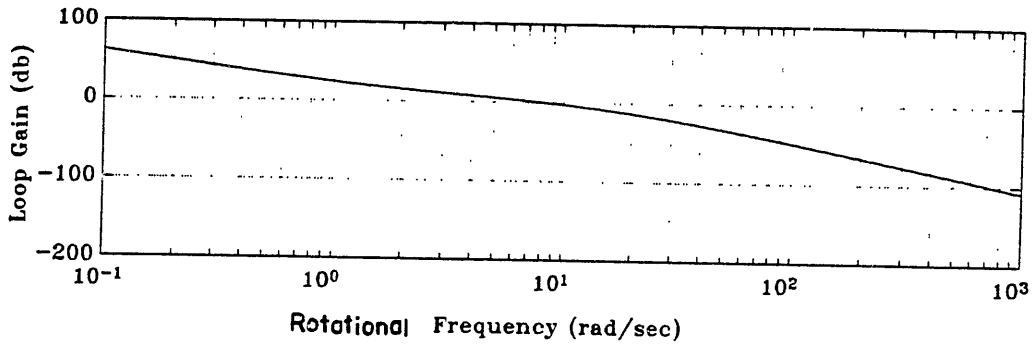

Figure 6.4. Loop Gain from Position Reference to Mass Center, Flexible Rotor (Soft Shaft), Bearing Feedback, Conventional Controller

frequencies, for which the gain G_cG_b is very small, the gain of P_n is equal to G_n, the value of the notch depth (D). This result is consistent with the improvement in performance due to the notch filter for the rigid rotor system at high rotational frequencies.

Figure 6.2 shows that the amount of improvement is less than the full notch depth for rotational frequencies above the flexible frequency (ω_s) for which the gain G_cG_b is large. In this region, the term $G_nG_cG_b$ is less than unity but relatively large compared to G_n, therefore P_n is approximately equal to $G_n(1 + G_cG_b)$, a value greater than G_n. For the plant, controller and nominal notch filter used here, the value of P_n is shown in Figure 6.5 as a function of rotational frequency. Thus, the effectiveness of the notch filter is reduced for values of rotational frequency below the highest crossover frequency of loop gain from synchronous disturbance to bearing position (G_cG_b), shown in Figure 3.7 to occur at approximately 230 radian/second. It was mentioned in Chapter 5 that

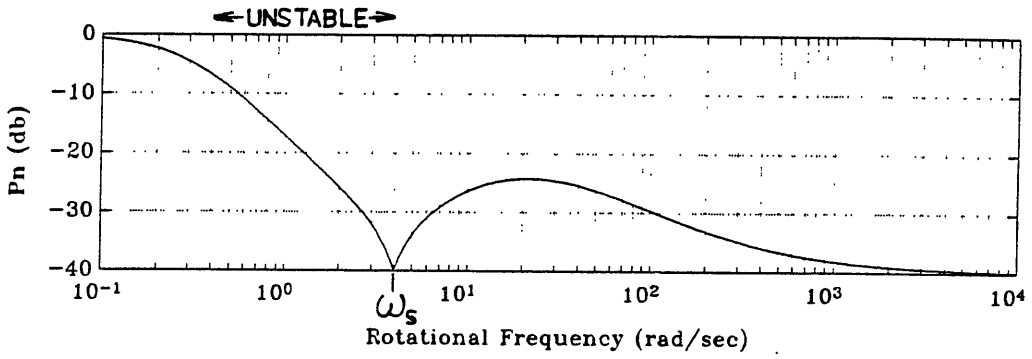

Figure 6.5. Notch Filter Controller Effectiveness, Soft Shaft, Bearing Feedback

increasing this crossover frequency was undesirable. The reason is that it reduces the notch filter effectiveness for rotational frequencies below this crossover frequency.

To summarize the flexible rotor system with rotor feedback, the range of unstable rotational frequencies lies roughly between the lowest crossover frequency of synchronous loop gain and the lowest critical frequency. The range of rotational frequencies for which the notch filter improves the system synchronous response lies above the lowest critical frequency, in the case of a soft shaft, above the flexible frequency (ω_s). For rotational frequencies above the highest crossover frequency of bearing position, the notch filter performance in attenuating the synchronous disturbance approaches the notch depth. Thus the useful range of rotational frequencies of the notch filter controller lies above the lowest critical frequency. The level of notch filter performance depends on the loop gain of bearing position (reference Figure 3.7).

6.2.2. Rotor Position Feedback

The stability and performance are enhanced by using

rotor position feedback because it reduces the complexity of the flexible rotor plant to the level of the rigid rotor model. The synchronous closed loop gain of this system from mass imbalance forcing function to center of mass position is given in Figure 6.6 both with and without the nominal notch filter. It shows that the notch filter effectiveness in reducing the synchronous response of the mass center exists for rotational frequencies above the crossover frequency of synchronous loop gain and is equal to the notch depth. From the previous chapter however, the unstable region extends from the synchronous loop gain crossover frequency to the loop gain crossover frequency (ω_c). Therefore the useful range of rotational frequencies with rotor feedback lies above the loop gain crossover frequency (ω_c).

An advantage of rotor position feedback is that it makes notch filter performance independent of G_b and the highest crossover frequency of bearing position. Notch performance is always equal to the notch depth. Rotor feedback also eliminates some mechanisms of synchronous disturbance by measuring the position closer to the actual center of mass. As discussed in the previous chapter, the stability using rotor feedback is also improved, however the effects of spillover must be considered.

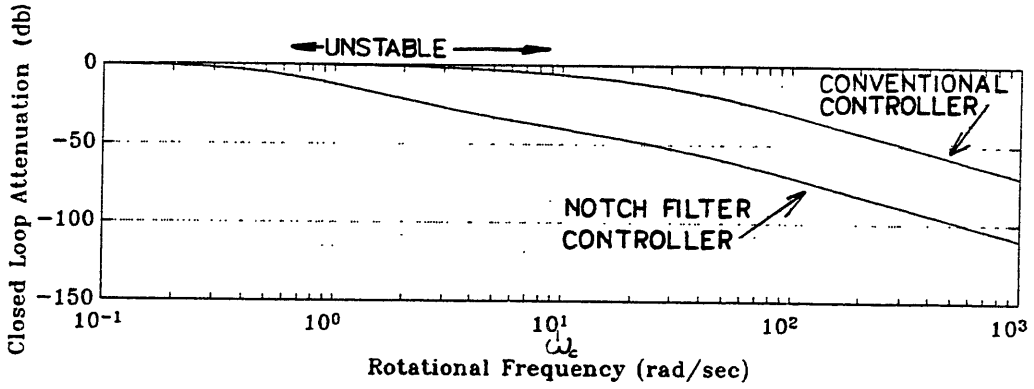

Figure 6.6. Synchronous Closed Loop Gain, Flexible Rotor (Soft Shaft), Rotor Feedback, Conventional and Notch Filter Controllers

CHAPTER 7
SUMMARY AND CONCLUSION

This thesis has examined the effects of a tracking notch filter controller on system stability and performance in reducing rotor response to the synchronous forcing function caused by mass imbalance. The approach has been to design conventional PID controllers for the different rotor models and then to examine the changes in stability and performance caused by the addition of a tracking notch filter to the conventional controllers. This chapter will summarize the approach and the results from each of the rotor models and present general conclusions based on the combined results.

To summarize the goal of the tracking notch filter controller, radial vibrations caused by rotor imbalance can be minimized by not allowing the bearings to produce forces at the rotational frequency. The notch filter attenuates the position feedback signal at this frequency to permit the rotor to spin about its center of mass, thus eliminating the source of these radial vibrations. Conventional controllers were designed to act on bearing position feedback for the three rotor models used. These models include a rigid rotor model, a flexible rotor model with a stiff shaft relative to the bearings, and a flexible rotor model with a soft shaft relative to the bearings. A controller was also designed to act based on rotor position feedback for the flexible rotor model with soft shaft.

The effect on system stability of the tracking notch filter was found to be a function of rotational frequency. Generally, the notch filter caused the system to become unstable between the lowest crossover frequency of synchronous loop gain, i.e. the loop gain evaluated at the rotational frequency, and the lowest critical frequency of the loop. The rigid rotor system has only one critical frequency at the loop gain crossover frequency (ω_c), which

is a function of rotor mass and bearing flexibility. The flexible rotor model in which the shaft is relatively stiff compared to the bearings is also unstable for rotational frequencies just below the crossover frequency of loop gain (ω_c), since this frequency is lower than the other critical frequency, the shaft flexible frequency (ω_c). The flexible rotor system in which the shaft is relatively flexible compared to the bearings becomes unstable over a range of rotational frequencies below the shaft flexible frequency, since this frequency is below the loop gain crossover frequency in this case. The use of rotor position feedback for the rotor model with a soft shaft showed stability characteristics similar to the rigid rotor system because the shaft flexible frequency is not a critical frequency in the loop transfer function of this system.

Performance of the notch filter in increasing attenuation of the synchronous forcing function caused by mass imbalance was evaluated for all the rotor models discussed. Generally, the conventional control systems provide attenuation for rotational frequencies above the lowest critical frequency. The notch filter controller provides additional attenuation at rotational frequencies above the lowest crossover frequency of synchronous loop gain. However, since the range of rotational frequencies between the synchronous loop gain crossover frequency and the lowest critical frequency cause unstable operation, a useful range of the notch filter controller was found as existing for rotational frequencies above the lowest critical frequency. Generally, the notch filter controller increases the attenuation in its useful range of rotational frequencies by approximately the notch depth. The exception to this is the system with soft shaft and bearing position feedback. In this case, the improvement in attenuation is less than the full notch depth for values of rotational frequency over which bearing gain (G_b) is not attenuated. The lightly damped poles at the flexible

frequency prohibit reducing the bearing gain in the useful range without reducing the damping of these poles and causing the system to oscillate at the flexible frequency. Note that this is a characteristic of the conventional controller, not the notch filter.

The advantage of rotor feedback control of the soft shaft rotor system is that the effects of shaft flexibility do not have an impact on stability or performance. There are no lightly damped poles at the flexible frequency and the improvement in notch performance is always equal to the notch depth in the useful range. Furthermore, the useful range of the notch filter controller can be chosen by changing the loop gain or bearing stiffness, and is not imposed by the plant. However, since the rotor position sensor and bearing actuator are not colocated, other shaft flexible modes may be destabilized, referred to as spillover effects.

Increasing the notch depth gives additional attenuation in the useful range of rotational frequencies, but it also increases the range of unstable rotational frequencies by reducing the crossover frequency of synchronous loop gain. Since a rotor system with magnetic bearings is likely to undergo transient changes in rotational speed, passing through the unstable range of frequencies would be necessary. The obvious solution to this problem is to disable the tracking notch filter below its useful range of rotational frequencies, since it serves no purpose there. The notch filter is enabled for rotational frequencies above the lowest critical frequency to attenuate the synchronous forcing function caused by mass imbalance. Handling the unstable range of rotational frequencies in this manner, a very deep notch filter may be chosen for its performance advantage without regard to its effect on increasing the unstable range of frequencies. It was shown that notch steepness, or Q factor, would have little effect on stability, therefore it can be chosen to

optimize bearing response to frequencies neighboring the synchronous frequency.

Tracking notch filter controllers are currently being used in conjunction with magnetic bearings to attenuate synchronous vibrations caused by rotor imbalance. Furthermore, previous research has shown that the notch filter causes the system to become unstable for rotational frequencies near critical frequencies of the system and that the notch filter must be disabled for these ranges of rotational frequencies. The goal of this thesis has been to provide a more thorough understanding of the mechanism by which the tracking notch filter attenuates the synchronous vibrations caused by rotor imbalance and how the stability of the system changes with rotational frequency. The contribution of this thesis is in defining the range of unstable rotational frequencies and how the dynamics of rotor, shaft and controller affect the performance of the notch filter.

Bibliography

[Beams, 1946] Beams, J.W. "The Production of High Centrifugal Fields". **Journal of Applied Physics**, Vol. 17, pp. 886-890, November, 1946.

[Downer, 1986] Downer, J.R. "Design of Large-Angle Magnetic Suspensions". Doctoral Thesis, Massachusetts Institute of Technology, May 1986.

[Earnshaw, 1842] Earnshaw, S. "On the Nature of the Molecular Forces Which Regulate the Constitution of the Luminiferous Ether". **Transactions of the Cambridge Philosophical Society.** 7 (1984): 97-112.

[Geary, 1964] Geary, P.J. **Magnetic and Electric Suspensions.** SIRA Survey of Instrument Parts, n6. Chiselhurst, Kent: British Scientific Instrument Research Association, 1964.

[Gunter, 1966] Gunter E.J. **Dynamic Stability of Rotor-Bearing Systems.** Washington D.C.: NASA, 1966.

[Habermann, 1984] Habermann, H., M.Brunet. "The Active Magnetic Bearing Enables Optimum Control of Flexible Rotor". ASME International Gas Turbine Conference. No 84-GT-117. 1984.

[Habermann, 1985] Habermann, H., M.Brunet. "The Active Magnetic Bearing Enables Optimum Control of Machine Vibrations". ASME International Gas Turbine Conference. No 85-GT-221. 1985.

[Huelsman, 1971] Huelsman, L.P., J.G.Graeme, G.E.Tobey. **Operational Amplifiers Design and Application.** Burr Brown Research Company. 1971.

[Jeffcott, 1919] Jeffcott, H.H. "The Lateral Vibrations of Loaded Shafts in the Neighborhood of a Whirling Shaft-The Effect of Want of Balance". **Philosophy Magazine** 6, n 37 (1919): 304-314.

[Johnson,1985] Johnson, B.G. "Active Control of a Flexible Rotor". Master's Thesis, Massachusetts Institute of Technology, January 1985.

[Johnson,1986] Johnson, B.G. "Active Control of a Flexible Two-Mass Rotor: The Use of Complex Notation". Doctoral Thesis, Massachusetts Institute of Technology, September 1986.

[Loewy, 1969] Loewy, R.G. **Dynamics of Rotating Shafts.** The Shock Vibration Information Center, Naval Research

Laboratory, Washington D.C., 1969

[Nikolajsen, 1979] Nikolajsen, J.L., R.L.Holmes, V.Gondhalekar. "Investigation of an Electromagnetic Damper For Vibration Control of a Transmission Shaft". **Proceedings of the Institution of Mechanical Engineers.** 193,(1979): 331-336.

[Ogata 1970] Ogata, K. **Modern Control Engineering.** Englewood Cliffs, NJ: Prentice-Hall, Inc. 1970.

[Salm 1984] Salm,J., G.Schweitzer. "Modelling and Control of a Flexible Rotor with Magnetic Bearings". **Proceedings of the Third International Conference on Vibrations In Rotating Machinery**, University of York, England: September 11-13, 1984, p.53.

[Weise, 1985] Weise, D.A. "Active Magnetic Bearings Provide Closed Loop Servo Control for Enhanced Dynamic Response". IEEE Machine Tool Conference. 1985

[Weise, 1987] Weise, D.A. "Present Industrial Applications of Active Magnetic Bearings". **22nd Intersociety Energy Conversion Engineering Conference.** Magnetic Bearings Inc., 1987.

Notation

B	Bearing center on the rotor disk
C	Output of generic transfer function
C_b	Center of bearing force
c_s	Shaft internal damping
D	Depth of notch filter
e	2.7183
E_b	Shaft elastic axis at bearings
E_r	Shaft elastic axis at rotor
F	Characteristic equation
F_s	Shaft force applied to rotor
F_b	Bearing force applied to shaft
F_x	Bearing force in x direction
F_y	Bearing force in y direction
G	Feed forward transfer function
G_b	Rotor transfer function F_b to Z_{Sb}
G_{cl}	Closed loop transfer function
G_{cls}	Synchronous closed loop transfer function
G_l	Loop transfer function
G_{ls}	Synchronous loop transfer function
G_m	Rotor transfer function F_b to Z_M
G_n	Notch filter transfer function
H	Feedback transfer function
j	Square root of -1
k_s	Shaft spring constant
m	Rotor mass
M	Rotor center of mass
M'	Rotor center of mass projected on bearing
n	Integers greater than 0
N	Number of clockwise encirclements of origin
P_n	Notch filter performance of soft shaft plant
Q	Notch filter steepness
R	Input of generic transfer function
s	Complex Laplace variable

S	Rotor elastic center
S_b	Bearing center of measurement
t	Time
x	Horizontal coordinate perpendicular to y
y	Horizontal coordinate perpendicular to x
z	Vertical coordinate
Z	Complex coordinate
Z_{Cs}	Complex position bearing force center
Z_M	Complex position mass center
Z_{Eb}	Complex position shaft elastic axis, bearing
Z_{Er}	Complex position shaft elastic axis, rotor
Z_S	Complex position measurement center,rotor
Z_{Sb}	Complex position measurement center, bearing
α_s	Phase angle, measurement center
α_b	Phase angle, bearing center of force
β	Phase angle, mass and elastic centers
δ	Shaft deflection distance
ϵ	Mass imbalance distance rigid rotor
ϵ_b	Bearing center of force misalignment
ϵ_c	Complex imbalance distance
ϵ_r	Mass imbalance distance, flexible rotor
ϵ_s	Measurement center misalignment
ω	Frequency
ω_1	Frequency at which notch gain is -3db
ω_2	Frequency at which notch gain is -3db
ω_o	Notch filter center frequency
ω_s	Shaft flexible frequency
Ω	Rotational speed
π	3.1416
ξ_d	Notch filter denominator damping factor
ξ_n	Notch filter numerator damping factor

Appendix A
Modified Nyquist Plot

This appendix details the modifications made to the Nyquist Stability criterion in order to make Nyquist plots more easily generated by computer. A short summary of the Nyquist stability criterion is necessary to show that the modified version gives the same results.

Nyquist Stability Criterion

Consider a system whose closed loop transfer function is:

$$\frac{C(s)}{R(s)} = \frac{G(s)}{(1 + G(s)H(s))} \qquad A.1$$

For stability, the roots of the characteristic equation,

$$F(s) = 1 + G(s)H(s) = 0 \qquad A.2$$

must all lie in the left half s plane. The Nyquist stability criterion relates the open loop frequency response, G(s)H(s), to the number of closed loop poles and zeroes which lie in the right half s plane.

For a given continuous closed path in the s-plane which does not go through any singular points, there exists a corresponding closed curve in the F(s) plane where F(s) is the characteristic equation defined in equation A.2. The relationship between the contour in the s-plane and the F(s) plane is said to be a conformal mapping. The number of poles and zeroes in the s plane enclosed by the contour determine the number and direction of encirclements of the origin in the F(s) plane. The total number of clockwise encirclements, N, of the origin of the F(s) plane, as a contour in the s plane is made in the clockwise direction, is equal to the number of zeroes minus the number of poles

of F(s) inside the contour in the s plane. This is called the mapping theorem.

The Nyquist criterion is the mapping theorem applied to control systems. The contour in the s plane encloses the entire right half plane. The number of clockwise encirclements of the point (-1 + 0j) in the G(s)H(s) plane is equivalent to N. In other word, a system must have the same number of counterclockwise encirclements of (-1 + 0j) as there are open loop poles in the right half s plane, otherwise the system is unstable.

For an open loop transfer function with a factor $1/s^n$ (where n = 1,2,3,...), the contour in the s plane excludes the origin by tracing a semicircle of infinitesimal radius around it. The corresponding plot of G(s)H(s) has n clockwise semicircles of infinite radius. In the s-plane, the contour approaches the origin along the negative imaginary axis and takes a right turn to begin its semicircle around the origin. This maps to a contour in the G(s)H(s) plane approaching infinity and making a right turn to begin n semicircles around the origin. This is because angles are preserved in conformal mappings.

Modified Nyquist Plot

The Nyquist stability criterion provides insight to control problems but the Nyquist plot is often difficult to generate when it extends to infinity. For the purpose of condensing this information closer to the origin and maintaining the significance of the point (-1 + 0j), G(s)H(s) is plotted on a different set of axes. The new axes defined on and outside the unit circle are 1 + log (base 10) of the real and imaginary parts of G(s)H(s) (e.g. the coordinates of the point (10 + 0j) becomes (2 + 0j)); inside the unit circle, the axes remain the same. Since the point (-1 + 0j) has not changed location, the significance of encirclements of this point is maintained. This plot can be used to determine system stability but

care must be taken when reading gain or phase information from it since the scales may be confusing.

Appendix B
Closed Loop Synchronous Frequency Response

The transfer function of a rotor system is generally a function of both frequency and rotational frequency, $G_r(s,\Omega)$. Consequently, the loop transfer function of an active magnetic bearing-rotor control system is a function of frequency and rotational frequency;

$$G_l(s,\Omega) = GH \qquad B.1$$

where G represents the feedforward transfer function and H represents the feedback transfer function and is assumed to be unity here. When the synchronous behavior of this system is of interest, the loop transfer function may be evaluated at the rotational frequency to give the synchronous loop transfer function,

$$G_{ls}(\Omega) = G_l(s,\Omega)\big|_{s=j\Omega} \qquad B.2$$

The closed loop transfer function of this control system is given as;

$$G_{cl}(s,\Omega) = \frac{G_l}{1 + G_l} \qquad B.3$$

Likewise, the closed loop transfer function may be evaluated at the synchronous frequency to give the synchronous closed loop transfer function;

$$G_{cls}(\Omega) = G_{cl}(s,\Omega)\big|_{s=j\Omega} \qquad B.4$$

The synchronous closed loop transfer function may also be defined as;

$$G_{cls}(\Omega) = \frac{G_{ls}}{1 + G_{ls}} \qquad B.5$$

In other words, the synchronous closed loop transfer function is a function of the synchronous loop transfer function (equation B.5), just as the closed loop transfer function is a function of the loop transfer function (equation B.3). The synchronous closed loop transfer function is the synchronous response of the system, i.e. the degree to which the output responds to the synchronous disturbance caused by mass imbalance. The synchronous loop transfer function is useful in estimating the value of the synchronous closed loop gain. When synchronous loop gain is above unity, the synchronous closed loop gain is unity and the system follows the synchronous disturbance. However, when synchronous loop gain is attenuated, synchronous closed loop gain has approximately the same shape and the output does not respond to the synchronous disturbance.